Technical Report 221

A STUDY OF STRATOSPHERIC EMITTERS BASED ON INFRARED RADIOMETERSONDE MEASUREMENTS

By
Maj Serhij Pilipowskyj, USAF
Hqs, Air Weather Service
and
Prof James A. Weinman
University of Wisconsin

PUBLISHED BY
AIR WEATHER SERVICE (MAC)
UNITED STATES AIR FORCE
AUGUST 1971

PREFACE

The problem of aerosols in the lower stratosphere has been of interest to meteorological physicists ever since the optical effects of volcanic dusts from giant eruptions were noted in the last century. The diffusion of such dusts suggested something about the stratospheric circulation, but investigational interest in stratospheric diffusion awaited the post-WW II age of nuclear weapons and the more direct measurements of conditions in the stratosphere. Observations of the infrared radiation flux in the atmosphere indicate an important influence of the aerosol distribution on the transmissivity characteristics of the atmosphere at these wavelengths. Thus, the stratospheric aerosol not only serves as a tracer for circulation studies, but is a factor in the application of certain optical techniques of geophysical, astronomical, astronautic, and military interest. The present study was undertaken in an effort to find a method of inferring the aerosol-emitter profile from infrared flux measurements by the Suomi-Kuhn radiometersonde, and to determine the global distribution of these emitters. These recent measurements of the stratospheric aerosol can serve as benchmarks for study of the possible stratospheric contamination effects of supersonic aircraft, missiles, rockets, etc. Since soundings with this instrument are relatively inexpensive and frequently made, their use for aerosol detection could have many practical applications.

The major part of this investigation was carried out by Major S. Pilipowskyj, and was accepted for fulfillment of requirements for the PhD degree at the University of Wisconsin. Prof. J. A. Weinman provided much assistance and general supervision of the project, which was primarily supported by funds from NSF Grants GA-888 and GA-11433, as well as from ESSA Grant WB-27 and Air Force OSR Grant 616-66.

The authors gratefully acknowledge constructive criticisms offered by Professors D. R. Johnson, C. Stearms, and E. Wahl, as well as by Major Pilipowskyj's co-workers at Hq Air Weather Service. Thanks are due to Dr. P. M. Kuhn of ESSA (now NOAA) for providing most of the radiometersonde data used, to Dr. R. W. H. Wright for his group at University of the West Indies for providing the LIDAR data, and to Dr. J. T. Peterson for his assistance in programming the Mie-theory computations.

Maj. S. Pilipowskyj, USAF
Dr. J. A. Weinman
15 March 1971

DISTRIBUTION: "F" plus Special

A STUDY OF STRATOSPHERIC EMITTERS BASED ON INFRARED RADIOMETERSONDE MEASUREMENTS

ABSTRACT

Analysis of downward-directed infrared irradiances measured in the lower stratosphere indicated that reasonable limits on the gaseous components of the atmosphere were not able to account for the irradiances observed between 14 and 24 km. Additional emitters were therefore assumed to exist at these altitudes. The altitude dependence of the additional emitter compared reasonably well with aerosol profiles derived from LIDAR backscatter measurements conducted simultaneously in the same region. Mie theory was applied to model aerosol size-distributions and, on the basis of the infrared and LIDAR data, estimates of the size distributions and mass density of the stratospheric aerosol at altitudes of ≈ 18 km were obtained.

Information on the spatial and temporal distributions of the stratospheric emitter was obtained from an analysis of some 400 measurements taken during the 1962-1967 period. The results indicate that while this phenomenon is global in scope, it is most evident in the tropics at altitudes between 15 and 18 km. In the mid-latitudes the emitter was found at about the same height, but the mean concentrations were only about 20% of those observed in the tropics. In Antarctica, the maximum mean concentration was 60% of that observed in the tropics and was located at an altitude of 20 km. The altitude at which the emitter was detected most frequently was generally between 15 and 18 km in the tropics and about one kilometer higher in the mid-latitudes. In Antarctica, the greatest frequency of occurrence was found at altitudes above 20 km.

Time series of daily radiometersonde ascents carried out during the Line Islands Experiment indicated that the emitter has a high persistence in the tropics. A series of synoptic-scale ascents made over the central United States on one night indicated that the emitter has a great variability in the mid-latitudes.

An analysis of mean seasonal distributions of the emitter was carried out for tropical, mid-latitude, and polar locations. Comparisons with mean seasonal circulation patterns of the stratosphere were carried out and indicate that the emitter is formed in the tropics and transported poleward along isentropic surfaces. Adiabatic heating taking place in such transport would result in higher air temperatures which would cause some of the emitters to evaporate, accounting for the decreased concentrations observed in the mid-latitudes. Attempts to relate the distribution of the emitters to synoptic circulation patterns were not successful.

No long-term trends in the concentration of the emitter in the tropics or in the mid-latitudes could be determined. There is some evidence, however, that an increase in the emitter concentration occurred over Antarctica from 1962 to 1964. This increase may be related to the Agung volcano eruption of 1963.

TABLE OF CONTENTS

LIST OF ILLUSTRATIONS

A STUDY OF STRATOSPHERIC EMITTERS BASED ON INFRARED RADIOMETERSONDE MEASUREMENTS

SECTION A — INTRODUCTION

Aerosols have been recognized as a significant atmospheric constituent for a number of years. Prior to the 1950s, however, little quantitative information existed on its vertical distribution, size, and composition. The general impression, supported primarily by searchlight probing techniques [13], was that the aerosol decreased exponentially with height, becoming a relatively insignificant scattering component when compared to Rayleigh scattering at altitudes above 15 km. Rosenberg [48] also supported the exponential decrease model, but concluded that the scattering due to aerosols was approximately equal to that from the molecular atmosphere for $\lambda = 0.5\ \mu$.

Since the eruption of Krakatoa in 1883, scientists have been aware that volcanic dust could be injected into the lower stratosphere to form layers of sufficient optical depth, on a global scale, so as to result in spectacular twilight phenomenon over most of the earth. Meteorologists took advantage of these volcanic ash clouds to infer wind speeds and circulation patterns at altitudes from 17 to 32 km. The spread of the Krakatoa dust cloud as related to the stratospheric circulation was discussed by Wexler [57]. Lettau [33] [34] treated the dust cloud in relationship to atmospheric diffusion processes and the dynamics of the equatorial atmosphere.

It was only in the late 1950s, when the distribution of radioactive debris in the atmosphere had become an item of interest, that a permanent layer of stratospheric aerosol was discovered by Junge [22], using balloon-borne impactors. During the past ten years, the existence of this layer has been verified by a number of direct and indirect techniques. In addition to the impactors used on balloons or airplanes [2] [38], in-situ measurements have been obtained by photoelectric particle counters [47] and by electric-field measurements [27] [44]. Scattered light radiation measurements aloft have been obtained from a rocket by deBary and Rossler [9] and from a balloon by Newkirk and Eddy [43]. Photography of the earth's limb from a spacecraft [11] has also been employed with some success to obtain the stratospheric aerosol profile.

Kondratiev [24] and Kosters [25] have employed measurements of the extinction of solar radiation in the atmosphere to obtain vertical profiles of the aerosol using balloon-borne instrumentation. By a rather complex method of photometry of twilight sky brightness, Volz [54] [55] has obtained low-resolution vertical profiles of the stratospheric aerosol. Elterman [14] has continued his searchlight studies. In the mid 1960s, technological developments provided a

unique new tool for probing the upper atmosphere for dust; the laser radar, or LIDAR. A number of studies of the stratospheric aerosol have been carried out using this tool, most noteworthy being those of Grams and Fiocco [19], Clemesha, et al. [4], and Collis and Ligda [6].

Inferences about aerosol concentrations obtained from impactor and optical techniques suffer serious shortcomings. The impactor efficiencies, especially for particles smaller than 0.2 μ in radius, may be questionable. The optical techniques depend on certain assumptions about the index of refraction and size distribution of the aerosols to obtain the absolute concentrations. Furthermore, the optical techniques are insensitive to the presence of particles smaller than 0.1 μ in radius. Thus, the results obtained from optical and impactor data may not adequately describe the small-particle aerosol. This small-particle aerosol has only a minor influence on optical phenomenon, but because the aerosol mass significantly affects infrared radiative transfer processes of the lower stratosphere, the infrared radiation may be used to detect the presence of such small particles.

A method is considered in this study to obtain vertical profiles of this small-particle aerosol from measurements of the radiation field which is most affected by it; namely, the downward infrared irradiance in the 3-μ to 90-μ region. By an analysis of the downward component of the infrared irradiance, which has been obtained from the Suomi-Kuhn net radiometer, the emitter profile in the 12-km to 25-km region can be inferred. The results are compared with LIDAR soundings, and a climatology based on some 400 radiometersonde soundings from various locations, obtained during the 1962-1965 period, is presented. Attempts are made to relate stratospheric dynamics with the emitter distributions, and a mechanism for the formation and distribution of the aerosol is postulated. Attempts were also made to relate the observed emitter to volcanic eruptions and tropical storm activities, but the results are inconclusive.

SECTION B — INSTRUMENTATION AND DATA PREPARATION

The vertical profiles of the downward stream of the infrared irradiance have been obtained with the Suomi-Kuhn net radiometer. During the past 12 years this instrument has been widely utilized for studies of atmospheric radiative processes in the troposphere and stratosphere. Extensive literature has been published describing its capabilities and limitations. The basic radiometer equations can be found in a paper by Suomi and Kuhn [50], and updated constants for use with these equations are in a manual by Kuhn and Suomi [29].

The downward-directed infrared irradiance was selected for this study as the most logical element. At altitudes above 12 km, the downward-directed irradiance is smaller than the upward-directed irradiance; hence, any additional

contribution due to the aerosol, as seen against a very cold background, would be easier to detect. Furthermore, the downward-directed irradiance is not affected by horizontally inhomogeneous emitters such as clouds, which may come into the field of view of the instrument and decrease the upward irradiance. Such an effect might be erroneously interpreted as an attenuating layer at the altitude of the radiometer.

The accuracy of the instrument has been considered theoretically by Johnson [21], and measured experimentally by Bushnell and Suomi [1], Kuhn [28], and Darkow [8]. Using an older model of the radiometer, Bushnell and Suomi found a standard error of ± 0.0036 ly/min for an irradiance measurement; Darkow showed that the radiometer was capable of solving the fine vertical structure of the radiative field and that the accuracy was not affected by rapid changes of air temperature such as those encountered in the vicinity of the tropical tropopause. In the description of a newer model of the radiometer, Kuhn and Johnson [30] indicated that the response time of the instrument had been decreased from 48 to about 15 seconds, which should make the irradiance measurements even less susceptible to rapid temperature changes. The measured accuracy of the irradiance values cited by these authors have a random error of ± 0.0012 ly/min. In addition, errors in thermistor calibrations can introduce a bias error of ± 0.0050 ly/min. At altitudes above 14 km, however, this error remains relatively constant. Such a bias error is not critical to our analysis, as we will be concerned with the variation of the downward irradiance with height rather than with its absolute values.

A total of 296 irradiance profiles obtained with the new model radiometer were selected for analysis. Since it was also desired to compare these data with those obtained with the older version of the instrument, an intercomparison flight of these radiometers was held in May 1966 at Green Bay. The results (see Figure B-1 in Appendix B) showed that while the downward irradiances differed by a constant value, the slopes of the irradiances were almost identical and yielded the same aerosol profiles. On the basis of these results, an additional 87 profiles obtained during the 1962-1963 period were selected for analysis.

All flight data were processed to obtain the downward-directed infrared irradiance using a filtering technique described by Kuhn and Johnson [30]. Further smoothing was obtained by selecting the mean irradiances and temperatures for 5-mb slabs for altitudes from 50 mb to 5 mb, and 10-mb slabs from 200 mb to 50 mb. This additional smoothing was undertaken to assure that only the most significant variations of the irradiance were considered and that instrumental lag effects would be minimized. The ascent rate of the radiometersonde in the region of the tropical tropopause is about 6 mb/minute; the radiometer, with a time constant of less than 20 seconds, should have reached a new equilibrium condition in less than 6 mb after rising above the tropopause. This is well within the 10-mb resolution utilized for this region.

SECTION C — RADIATIVE TRANSFER MODELS APPLIED TO ATMOSPHERES CONTAINING ONLY OZONE, CARBON DIOXIDE, AND WATER VAPOR

It was first necessary to develop a radiative transfer model for this region of the stratosphere to determine the vertical aerosol profiles.

If a horizontally homogeneous atmosphere is in thermodynamic equilibrium, the irradiance $H_z^{\downarrow}$ at a reference level z is:

$$(1) \qquad H_z^{\downarrow} = \sum_{j=1}^{j=3} \int_0^{u_j(z)} \sigma T^4(u_j) \cdot \left(\frac{\partial \epsilon(u_j)}{\partial u_j}\right) \cdot du_j$$

where u_j is the optical depth of the emitting atmospheric constituent j, namely carbon dioxide, ozone, or water vapor. The optical path in gaseous absorbers depends on temperature and pressure in the manner described by Kuhn and Cox [31]. The slab emissivity of the constituent j is the ratio of emitted infrared irradiance to the blackbody irradiance at the same temperature.

$$(2) \qquad \epsilon(u_j) = H(u_j T)/\sigma T^4$$

Such emissivities were computed for the gaseous constituents in the manner cited by Elsasser and Culbertson [12]. Pressure broadening was assumed to be sufficiently negligible in the stratosphere, thus permitting neglect of the overlapping of absorption lines of the various gaseous constituents. The emissivity gradients of the individual constituents thus could be added to simplify the evaluation of the integral of Equation (1).

It is generally assumed that a knowledge of the air-temperature profiles, the vertical distributions of carbon dioxide (assumed uniformly mixed, 0.031% by volume), of ozone (which emits a small albeit variable fraction of the irradiance $H_z^{\downarrow}$), and of water vapor render it feasible to evaluate $H_z^{\downarrow}$ in Equation (1).

Ascents of frost-point hygrometer-sondes and radiometersondes were therefore made only hours apart in order to determine whether these three gaseous emitters could account for the measured irradiance $H_z^{\downarrow}$. The results of one of these flights, shown in Figure 1, carried out in Washington, D. C. on 23 May 1966, indicated that the stratosphere was dry. Computation of $H_z^{\downarrow}$ implied that it would require a tenfold increase in the measured water-vapor concentrations to produce the observed downward irradiance. This can be seen in Figure 1, which shows that the measured water-vapor concentration at 70 mb was 2.7×10^{-6} gm/gm, but a concentration of 22×10^{-6} gm/gm would be required to yield the measured infrared irradiance shown in Figure 2. Clearly some additional emitter must be present in the lower stratosphere to account for the observed values of $H_z^{\downarrow}$.

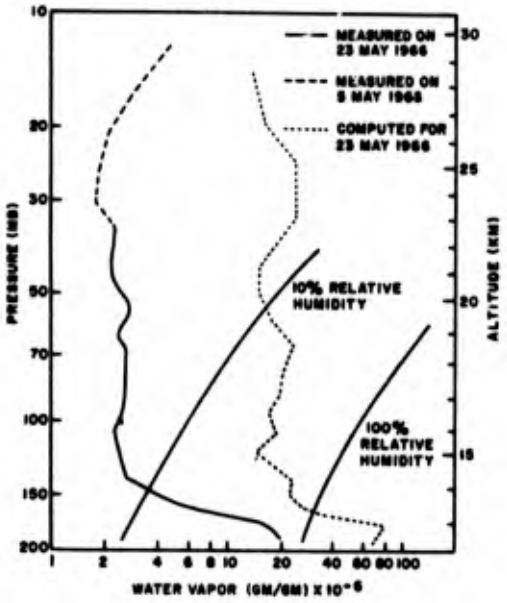

Figure 1. Measured and Computed Water-Vapor Concentrations over Washington on 23 May 1966 [36].

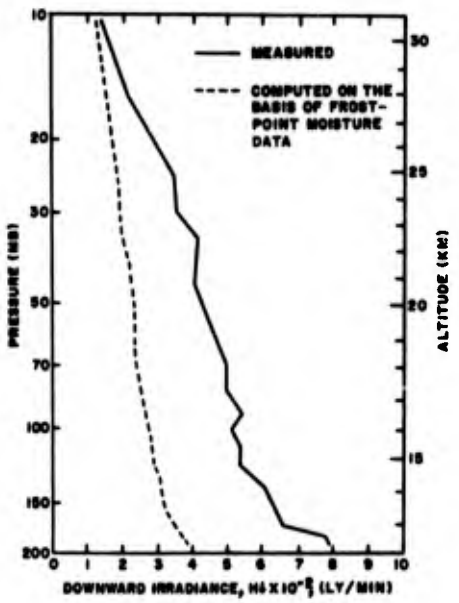

Figure 2. Measured and Computed Infrared Downward Irradiances Profiles over Washington on 23 May 1966.

SECTION D — INTERCOMPARISON WITH LIDAR DATA

An intercomparison between radiometersonde data and a LIDAR profile was conducted in order to determine whether the additional emitter was associated with the stratospheric aerosol.

Radiometersonde Measurements.

The procedure used to evaluate Equation (1) in the previous experiment was repeated. Water vapor is a significant emitter at altitudes exceeding 15 km; however, in this case, no direct measurement of this quantity was available. The water-vapor distribution models shown in Figure 3 were therefore postulated. These distributions represent "wet" and "dry" limits, and a "typical" representation derived from the measurements of Calfee and Gates [3], Houghton [20], Mastenbrook [36], Murcray [39] [40], and Zander [58]. A moisture profile measured by Mastenbrook [36] over Jamaica on 25 March 1965 is also shown in Figure 3.

Figure 4 shows the irradiance, $H_z^{\downarrow}$ averaged from measurements of three radiometersonde ascents conducted over Miami, Florida, from 31 March 1965 to 1 April 1965. The temperature profiles used in Equation (1), measured during the ascents, and the humidity profile measured during the hygrometer ascent were

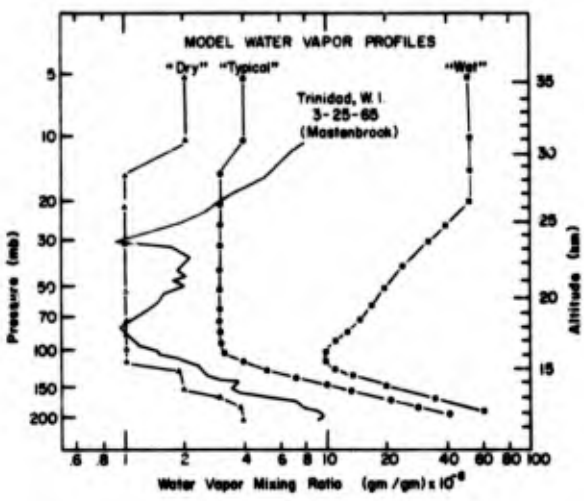

Figure 3. Models of Stratospheric Water-Vapor Distribution.

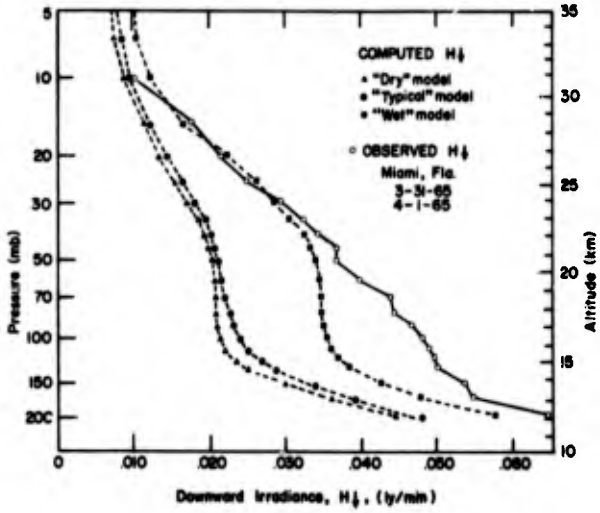

Figure 4. Measured and Computed Infrared Downward Irradiances Profiles over Miami.

incorporated in the evaluation of Equation (1). The temperature distribution cited by Cole, et al. [5] was used to evaluate Equation (1) for altitudes between 30 km and 50 km. Figure 4 also shows that the evaluation of Equation (1) using the "wet" water-vapor distribution is still insufficient to account for the measured irradiance $H\downarrow_z$ at 14 km $\leq z \leq$ 24 km.

A computer program was developed to add sufficient nongaseous emitters in the evaluation of Equation (1) to provide a calculated irradiance within 0.001 ly/min of the measured value. This accuracy is consistent with the random error of the data. It was postulated that there were no emitters above 30 km, that the emitter present in the 30 km - 12 km region was gray and that the amount of overlap between the gray-body emitter and the sharp spectral lines of the radiating gases was negligible. The gray-body infrared slab emissivity was assumed to be of the form [18]:

$$(3) \qquad \epsilon_z = 1 - \exp\left(-1.67 \int_z^\infty \beta_{abs}(z')\, dz'\right)$$

where $\beta_{abs}(z')$ is the absorption coefficient at an altitude z'.

The effect of the radiometer bias errors on the results was investigated and found to be very minor. This is because the calculated gray-body emissivity depends primarily on the rate of change of the irradiance with height, rather than on the absolute value of $H\downarrow_z$. On this basis it can be stated that the inferred value of β_{abs}(18 km) is accurate to $\pm 5 \times 10^{-8}$ cm^{-1}. The histograms of Figures 5 and 6 show $\beta_{abs}(z)$ computed in this manner from data obtained from

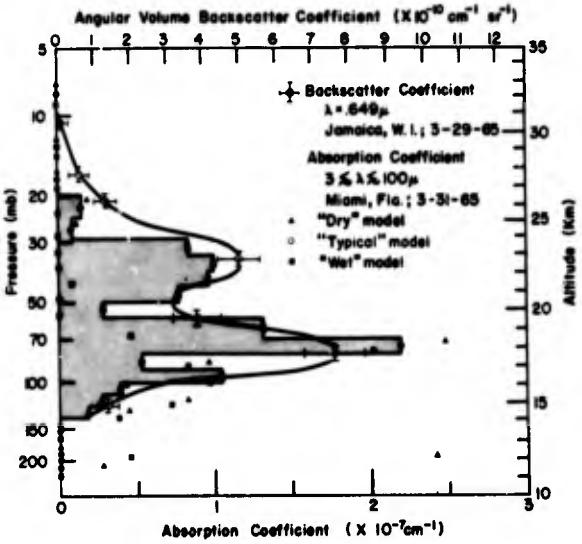

Figure 5. Computed Infrared Absorption Coefficients from Miami for 31 March 1965 and 1 April 1965, LIDAR Backscatter Profiles from Jamaica on 29 March 1965.

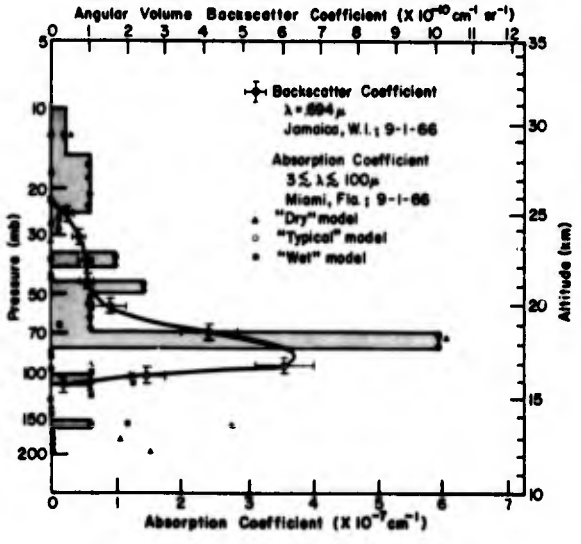

Figure 6. Computed Infrared Absorption Coefficients from Miami and LIDAR Backscatter Profiles from Jamaica on 1 September 1966.

radiometersonde ascents over Miami from 31 March 1965 to 1 April 1965 and on 1 September 1966, respectively. The shaded histograms show $\beta_{abs}(z)$ derived from calculations employing the "typical" water-vapor distributions. Results derived from the "dry" and "wet" distributions are also included.

LIDAR Measurements.

The pulsed-ruby LIDAR system described by Kent, et al [26] was utilized in this study to measure light ($\lambda = 0.69\ \mu$) scattered 180° by atmospheric constituents as a function of altitude. This equipment provides a measure of the scattering cross-section of the atmosphere at altitudes between 15 km and an upper limit of about 40 km by day and 70 km by night. Above 30 km the backscattered signal has at all times been found to vary with altitude in accordance with the theory that the scattering is entirely from atmospheric molecules. Below 30 km, and particularly between 14 and 24 km, an increased backscatter is observed, varying somewhat from day to day, which is attributable to aerosol scattering. As losses in the equipment and absorption in the lower atmosphere are difficult to measure, the apparatus is calibrated by assuming that the scattered signal from great heights is entirely that due to Rayleigh scattering from the atmosphere, with no additional aerosol component. This calibration is then used to compute the angular volume backscatter coefficient for the lower altitudes ($z \lesssim 30$ km). The resulting profiles obtained for the aerosol scattering once the Rayleigh scattering has been subtracted are shown in Figures 5 and

6. It should be noted that the backscattering coefficients obtained in this way represent lower limits on the backscatter coefficient of the aerosol.

Although the data and analyses which provide the infrared absorption coefficient and the $\lambda = 0.694\ \mu$ angular volume backscatter coefficient are subject to sizable uncertainties, the qualitative dependence on altitude of both of these quantities is quite similar. Both quantities shown in Figure 6 exhibit a 50% decrease at z = 20 km. This, therefore, confirms that these quantities are correctly determined within approximately 50%.

SECTION E — INFERENCES ABOUT EMITTERS

On the basis of the intercomparisons between the laser and radiometersondes, and on the basis of the calculations which show that it would require unreasonable concentrations of water vapor to obtain the observed downward irradiances, we will assume that the radiometersonde is detecting a nongaseous emitter.

Murcray [41] has suggested that HNO_3 vapor exists at altitudes where the aerosol layers are observed. On the basis of Murcray's recent measurements, Fried [16] estimates that the Planck gray-body absorption coefficient of HNO_3 for $3\ \mu < \lambda < 90\ \mu$ may be $\beta_{abs}(18\text{ km}) \simeq (3.6 \pm 1.3) \times 10^{-9}\text{cm}^{-1}$, a value considerably smaller than the measured $\beta_{abs}(18\text{ km})$ of $(4 \pm 2) \times 10^{-7}\text{cm}^{-1}$ shown in Figures 5 and 6. We will assume for the present analysis that the excess emitter is a gray body, and that it is presumably an aerosol, although it is possible that HNO_3 may, under some conditions, emit sufficient radiation to account for some of our observations.

The question of the size distribution of the aerosol which is postulated to account for the infrared and laser results has been examined by Pilipowskyj, et al. [45]. It was concluded that the laser and radiometersonde are not really looking at the same aerosol particles. While the laser detects particles predominately greater than 0.1 μ in size, the particles detected by the infrared technique may be less than 0.03 μ. This analysis, as well as an analysis of the mass concentration of the aerosol, is presented below:

Size Distribution #1.

Friend [17] found from direct sampling that the large aerosol has a size distribution that can be approximated by the analytical expression

$$(4)\qquad \frac{dN_1(r)}{d(\log r)} = \begin{cases} 4.58\ \bar{N}_1\ (r/0.3)^{4} & 0.1\ \mu \le r \le 0.3\ \mu \\ 4.58\ \bar{N}_1\ (r/0.3)^{-4} & 0.3\ \mu \le r \le 1.0\ \mu \end{cases}$$

where r is the particle radius in μ and $\bar{N}_1 = 0.066$ particles/cc.

A Mie-theory computer program utilizing the procedure of Deirmendjian,

Clasen, and Viezee [10] was applied to an ensemble of dielectric spheres with refractive index 1.5 and the size distribution of Equation (4) to calculate the angular volume backscatter coeffieient for $\lambda = 0.694\ \mu$ radiation:

$$(5) \qquad \underset{\lambda=0.694\mu}{f(180^\circ)} = \left(\frac{\lambda}{2\pi}\right)^2 \int_{0.1\mu}^{1.0\mu} i\left(180^\circ, \frac{2\pi r}{\lambda}\right) \cdot dN_1(r) = 1.83 \times 10^{-11}\ \text{cm}^{-1}\ \text{sterad}^{-1}$$

where $i(180^\circ, 2\pi r/\lambda)$ is the intensity of light scattered 180° by a homogeneous sphere of radius r with index of refraction n = 1.5. This result is inadequate to account for the angular volume backscatter coefficient measured at an altitude ≃ 18 km, namely

$$\underset{\lambda=0.694\mu}{f(180^\circ)} = (7 \pm 2) \times 10^{-10}\ \text{cm}^{-1}\ \text{sterad}^{-1}$$

Although Friend [17] found no variation in $\bar{N}_1$ with latitude, Rosen [47] observed an aerosol concentration in the tropics 5 to 10 times greater than that observed at higher latitudes. Such regional variations in $\bar{N}_1$ have sometimes been invoked to account for discrepancies between directly sampled data and optical measurements.

The infrared absorption coefficient can be equated to the Planck mean opacity:

$$(6) \qquad \beta_{abs}(18\ \text{km}) = \frac{1}{\sigma T^4} \int_{0.1\mu}^{1.0\mu} \int_{3\mu}^{90\mu} \pi r^2\, Q_{abs}\left(\frac{2\pi r}{\lambda}, n, k\right) \cdot B_T(\lambda)\, d\lambda\, dN_1(r)$$

$$= 7.43 \times 10^{-11}\ \text{cm}^{-1}$$

where σ is the Stefan-Boltzmann constant, T ≃ 200°K is the temperature at z ≃ 18 km, $B_T(\lambda)$ is the Planck blackbody function, $dN_1(r)$ is obtained from Equation (4), and the infrared absorption efficiency factor is

$$(6a) \qquad Q_{abs} \simeq 24 \cdot n \cdot k \cdot \left(\frac{2\pi r}{\lambda}\right) / [(n^2 - k^2 + 2)^2 + 4n^2k^2]$$

when $\lambda > r$ [51]. Although the infrared indices of refraction of the stratospheric aerosol are not known, we may assume that n = k = 1.5. The value for n for the infrared is chosen in the same manner for the visible region (for example, the real index of refraction of water does not change markedly with λ).

The imaginary part of the index k is chosen to maximize Q_{abs} for a given n. In spite of this choice of k, the calculated absorption coefficient of Equation (6) is much smaller than the measured

$$\beta_{abs}(18\ \text{km}) = (4 \pm 2) \times 10^{-7}\ \text{cm}^{-1}$$

It is difficult to reconcile the drastic discrepancies between the measured radiative quantities and those computed from a size distribution derived from

the directly sampled data of Friend [17] even if one allows for temporal and spatial variations in the characteristics of the aerosol or if the collection efficiency of the sampling equipment had been overestimated.

Size Distribution #2.

Rosen [47] suggested that the size distribution of Equation (4) derived from impactor measurements does not accurately describe the stratospheric aerosol because volatile particles, which may be stable at altitudes exceeding 14 km, do not remain on the impactors when these are returned to earth. The aerosol size distribution may be represented by a power law

$$(7) \qquad \frac{dN_s(r)}{d(\log r)} = 2.31\, \nu\, \bar{N}_s \cdot \left(\frac{r}{r_{s_{min}}}\right)^{-\nu}$$

where r is the aerosol radius. Cutoff radii $r_{s\ max}$ and $r_{s\ min}$ are selected so that $r_{s\ max} > r > r_{s\ min}$ and $\bar{N}_s$ is then the total number of particles/cc in this size range.

Mie theory was applied to an ensemble of particles given by Equation (7) to evaluate $f(180°)_{\lambda=0.694\mu}$ and $\beta_{abs}(18\text{ km})$. Attempts were made to adjust $r_{s\ min}$, ν, and $\bar{N}_s$ so that the theory could yield the observed values of both $f(180°)_{\lambda=0.694\mu}$ and $\beta_{abs}(18\text{ km})$. Only $\nu \gtrsim 4.5$ could account for both measured quantities for $0.01\mu \leq r \leq 60\mu$. The result is inconsistent with the measurements of Newkirk and Eddy [43] and Rosen [47]. This disagreement is attributable to the fact that optical measurements are not as sensitive to aerosols with $r < 0.1\mu$ as are infrared measurements. If Mie theory is utilized only to derive an $f(180°)_{\lambda=0.694\mu}$ from size distribution (Equation (7) with $\nu = 2.5$ and $r_{s\ min} = 0.1\mu$, i.e., the values obtained by Newkirk and Eddy [43] and Rosen [47], then $\bar{N}_s = 5.2 \pm 1.5$ particles/cc. This compares favorably with $\bar{N}_s = 12 \pm 5$ particles/cc reported by Rosen [47].

Mie theory was applied to the size distribution Equation (7) with $\nu = 2.5$, $r_{s\ min} = 0.1\mu$, and $\bar{N}_s = 5.2 \pm 1.5$ particles/cc to yield

$$\beta_{abs}(18\text{ km}) = (5.8 \pm 1.7) \times 10^{-9}\text{cm}^{-1}$$

The size distribution Equation (7) is thus insufficient to account for the measured infrared $\beta_{abs}(18\text{ km})$.

Size Distribution #3.

Although the optical measurements can be explained by a power law aerosol size distribution Equation (7), which employs reasonable values of ν, $r_{s\ min}$ and $\bar{N}_s$, this size distribution cannot be adjusted to yield absorption coefficients as large as those observed. It is therefore necessary to postulate the existence of an additional ensemble of small aerosols with $r < 0.1\mu$ that scatter red light insignificantly in comparison with aerosols described by Equation

(7) but that absorb infrared radiation more than these larger aerosols. DeBary and Rossler [9] were also compelled to attribute the intensity of sunlight scattered from the stratosphere at various angles and wavelengths $\lambda = .40\mu$ and $.55\mu$ to abundant small aerosols with $r < 0.1\mu$.

The integral form Equation (6a) can be satisfied by any number of hypothetical size distributions, the "effective" size distribution of the additional small aerosol is therefore assumed to be

$$(8) \qquad \frac{dN_s}{d(\log r)} = \frac{\bar{N}_s}{\log (r_{s\ max}/r_{s\ min})}$$

i.e., a rectangular distribution; where $\bar{N}_s$ is the total number of particles per c.c. with radii $r_{s\ min} \leq r \leq r_{s\ max}$. Because $f(180°)_{\lambda=0.694\mu}$ is attributed primarily to large aerosols with $r \geq 0.1\mu$, only $f'(180°)_{\lambda=0.694\mu} = 10^{-1}\,°cm^{-1}\,sterad^{-1}$ is assumed to be caused by small aerosols with $r \leq 0.1\mu$. This reduced value, $f'(180°)_{\lambda=0.694\mu}$, is chosen because it does not cause a significant change in $\bar{N}_s$, the total large particle density derived from the LIDAR measurements only. The reduced $f'(180°)_{\lambda=0.694\mu}$ and the absorption coefficient $\beta_{abs}(18\text{ km})$ were re-evaluated from the Mie theory applied to an ensemble of particles described by the sum of Equations (7) and (8). The results were compared to the values of these quantities measured at 18 km. Although only two quantities were measured, it is possible to estimate $r_{s\ max}$, $r_{s\ min}$, and $dN_s/d(\log r)$ which simultaneously yield the measured $f'(180°)_{\lambda=-.694\mu}$ and $\beta_{abs}(18\text{ km})$. The minimum of particles required to produce the observed values of these parameters is

$$\frac{dN_s}{d(\log r)} \geq 10^{(7.8\ ^{+\ 0.6}_{-\ 0.4})} \quad \text{particles/cc}$$

The corresponding maximum radius is

$$r_{s\ max} \leq (1.3\ ^{+\ 0.2}_{-\ 0.3}) \times 10^{-2}\ \mu$$

The minimum radius

$$r_{s\ min} \simeq 3 \times 10^{-3}\ \mu$$

is determined by the fact that small aerosols coagulate rapidly [22]. Even if the entire $f(180°)_{\lambda=0.694\mu}$ had been employed to evaluate $r_{s\ max}$ and $dN_s(r)/d(\log r)$ rather than $f'(180°)_{\lambda=0.694\mu}$

$$dN_s(r)/d(\log r) \geq 10^{(6.9\ ^{+\ 0.6}_{-\ 0.3})} \quad \text{particles/cc}$$

and

$$r_{3\ max} = (2.4 \begin{smallmatrix} + 0.4 \\ - 0.5 \end{smallmatrix}) \times 10^{-2}\ \mu$$

would have been obtained.

Mass Density of Aerosol.

The mass density of aerosol can be derived from the infrared absorption coefficient if it is recalled from Equation (6) that

$$\beta_{abs}(z) \simeq A(\bar{\lambda},n,k) \bullet \int_0^{1.0\mu} \pi r^3 \bullet \left(\frac{dN_i}{dr}\right) dr$$

where $A(\bar{\lambda},n,k)$ is the coefficient of r in Equation (6a) and where

$$\bar{\lambda} = \sigma T^4 / \int_{3\mu}^{90\mu} \lambda^{-1} \bullet B_T(\lambda) \bullet d\lambda \qquad \text{and} \qquad dN_i/dr$$

may be any aerosol size distribution such that $r < \lambda$. The mass density of aerosol at altitude z is

$$(9) \qquad M(z) = \frac{4}{3} \rho \int_0^{1.0\mu} \pi r^3 \, (dN_i/dr)\, dr \gtrsim \frac{4}{3} \bullet \rho \bullet \beta_{abs}(z)/A(\bar{\lambda},n,k)$$

Thus, if the assumed bulk density of the aerosol is $\rho = 2$ gm/cc then,

$$M(18\ km) \gtrsim (14 \pm 7) \times 10^{-11}\ gm/cc$$

The cited value is a lower bound on the mass density of aerosol because k was chosen to maximize $A(\bar{\lambda},n,k)$ for $n = 1.5$.

The measurements of Figure 6 obtained between 31 March 1965 and 1 April 1965 are especially interesting. The analysis of Equation (9) was applied to these data to yield

$$M(18\ km) \gtrsim (8 \pm 2) \times 10^{-11}\ gm \bullet cc^{-1}$$

corresponding to a minimum mixing ratio $(6 \pm 2) \times 10^{-7}$ gm/gm. Similarly,

$$M(23\ km) \gtrsim (3 \pm 1) \times 10^{-11}\ gm \bullet cc^{-1}$$

corresponding to a minimum mixing ratio $(6 \pm 2) \times 10^{-7}$ gm/gm.

Comparing these mass density results with those obtained by others, we find some substantial disagreements. Mass densities reported by Rosen [46] and Grams and Fiocco [19] are more than one order of magnitude smaller than the mass den-

sity obtained at 18 km by the radiometersonde method. This disagreement may be explained, in part, by the fact that the optical techniques used by these authors are insensitive to the small-particle aerosol, which the analysis indicates may be a major constituent of the stratospheric aerosol.

The frost-point data obtained by Mastenbrook [36] over Trinidad, W. I., on 25 March 1965 are shown in Figure 3. The water-vapor mixing ratio exhibits minima at 18 and 23.5 km, each corresponding to a reduction of $\sim 10^{-6}$ gm/gm from the mixing ratio measured at adjacent altitudes. This is approximately equal to the mass of the aerosol at these altitudes and tempts one to speculate that the small aerosol has removed a significant amount of water vapor from the tropical stratosphere at these levels. However, a comparison of the moisture profile shown in Figure 1 with a vertical aerosol profile derived from the infrared irradiance measurements shown in Figure 2 does not indicate any such inverse correlation between the water vapor and aerosol during the Washington intercomparison.

It should be stressed again that the additional emitter required to account for $H_z^{\downarrow}$ could be a gas other than CO_2, O_3, or H_2O; for example HNO_3 vapor. This additional emitter also exists at the same altitudes as the aerosols which scatter the 0.694μ light [16].

SECTION F — CLIMATOLOGY OF THE STRATOSPHERIC EMITTER

The Data Base.

The 400-odd vertical profiles of the aerosol extinction coefficient which comprise the data base for the climatological analysis represent a rather non-homogeneous and possible biased sample. For these reasons, the term climatology may not be exactly appropriate. Nevertheless, since this study presents an attempt to analyze the seasonal and geographical distribution of this emitter, presenting the results in a climatological context may be justifiable.

The location and period of observations for the data are as follows:

Old radiometer (small disk, rod thermistor)

Byrd Station (80°S, 119°W) Apr-Sep 1962	32 ascents
Byrd Station (80°S, 119°W) Apr-Aug 1963	23 ascents
Hallett Station (77°S, 41°W) Apr-Oct 1963	14 ascents
Pole Station (90°S) Apr-Sep 1963	13 ascents
Wilkes Station (66°S, 110°E) Apr-Aug 1963	5 ascents

New radiometer (small disk, bead thermistor)

Byrd Station (80°S, 119°W) Apr-Sep 1964	43 ascents
Washington (30°N, 77°W) Oct 1964-Jul 1965	43 ascents
Miami (26°N, 80°W) Mar 1965-Sep 1966	7 ascents

Guam (14°N, 145°E) Oct 1964-Sep 1965	37 ascents
Canton Isl (2°S, 172°W) Oct 1964-Dec 1965	45 ascents
Christmas Isl (2°N, 158°W) 21 Mar-21 Apr 1967	20 ascents
Palmyra Isl (6°N, 161°W) 23 Mar-21 Apr 1967	21 ascents
Midwestern United States 12 Dec 1965	37 ascents

Byrd Station has the longest period of observations — three years. Because the radiometersonde cannot be used in daylight, only polar winter data are available. The same is true for the other Antarctic stations. Data for a complete annual cycle are available only for Guam and Canton Island. Washington data cover almost a full year, but the data for Green Bay span only the fall and winter periods.

A time series of daily observations was conducted at Christmas Island and Palmyra Island during the Line Island Experiment. Regrettably, there are several data gaps which make it difficult to establish a clear idea of the day-to-day variations of the emitter in the tropics.

The Miami data consist of a small sample over a short time period, and, in view of the variability of this data, it is questionable as to how well it represents a "typical" subtropical condition. The 12 December 1965 data for the midwestern United States represents a synoptic-scale look at the emitter.

Global Distribution.

The mean global distribution of the stratospheric emitter can be presented in two ways: as the distribution of the mean infrared absorption coefficient β_{abs}, which is assumed to be indicative of the emitter concentration (Figure 7),[1] or as a distribution of the frequencies of occurrence of detectable emissions assumed to be due to the aerosol (Figure 8). Both graphs are based on the same data, some 200 profiles obtained by the new model radiometer during the 1964-1965 period. The number of observations which went into each vertical profile is indicated under the station name in Figure 7 and at the top of Figure 8. The breaks in the isopleths are deemed necessary to indicate that the mean absorption coefficients along the 80°W meridian may not be identical to those at 180°W.

From these charts we see that there is a well-defined layer of infrared emitters extending from the tropics to the mid-latitudes. The maximum concentration of the emitter occurs at about 90 mb both in the tropics and in the mid-latitudes. There is a secondary layer located at about 100 mb in the vicinity of the intertropical convergence zone at about 15°N. In the mid-latitudes there is a hint of a secondary maximum at about 40 mb.

[1] In this figure, as in most others in this report, both height and pressure values are given. The emitter distributions were calculated with respect to the pressure coordinates. The height values, based on a US Standard Atmosphere, are included for the sake of convenience.

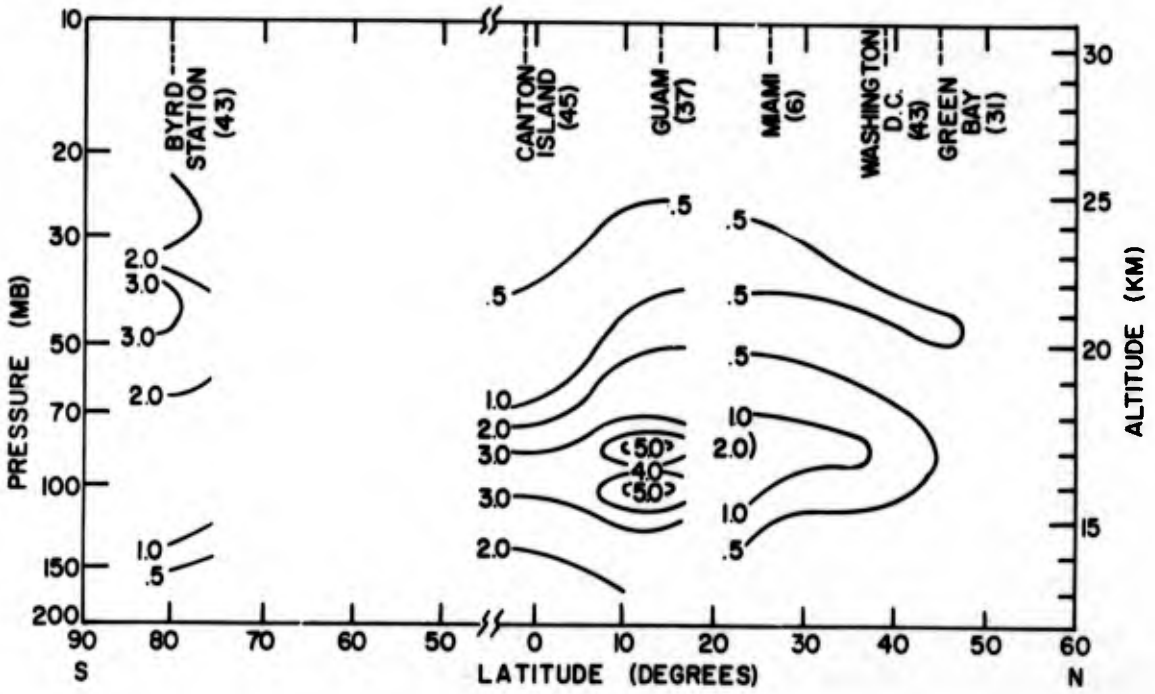

Figure 7. Latitudinal Cross-Section of the Mean Infrared Absorption Coefficient for April 1964-December 1965 Period ($\beta_{abs} \times 10^{-7} cm^{-1}$).

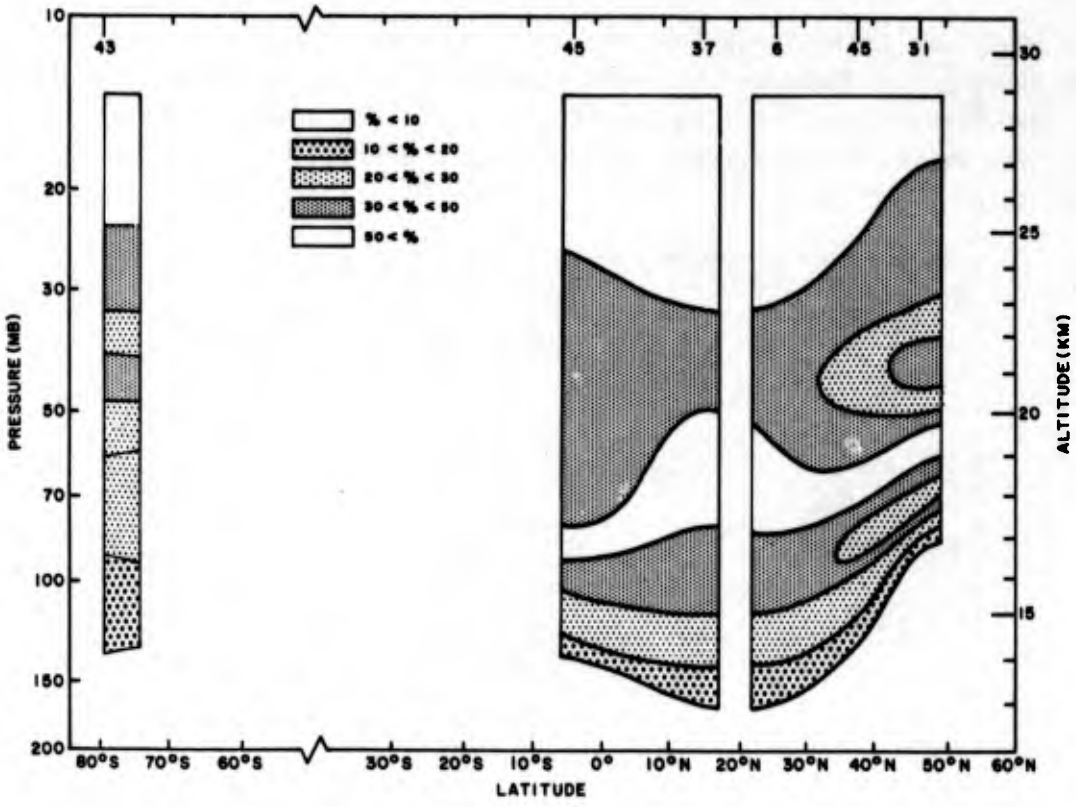

Figure 8. Latitudinal Cross-Section of the Frequency of Occurrences of Detectable Emitters for April 1964-December 1965 Period.

It is interesting to note that the absorption coefficient is almost one order of magnitude greater at 15°N then it is at 45°N, decreasing from 5×10^{-7} to $0.5 \times 10^{-7} cm^{-1}$ at 90 mb. The maximum absorption coefficient in Antarctica is $3 \times 10^{-7} cm^{-1}$ between 50 and 40 mb. It should be noted that the Antarctica data represent only the wintertime condition. The mid-latitude data at Green Bay are also biased, with most of the observations obtained during the winter months.

The frequency of occurrence shows a well-defined peak in the mid-latitudes at altitudes between 70 and 60 mb. The maximum values are about 50%. In the vicinity of 25°N, the maximum frequency of occurrence of more than 60% is near 60 mb and the layer is very diffuse with the 50% of occurrence isopleths extending from 90 to 50 mb. Near the equator, the layer once again becomes more sharply defined with the maximum of occurrence of 50% at 90 mb. In Antarctica, the maximum occurrence of 40% is at an altitude of 45 mb.

There is a pronounced minimum of occurrence of measurable emitters between 50 and 30 mb both in the mid-latitudes and in the tropics; in Antarctica this minimum occurs at about 35 mb. At altitudes above 25 mb there is an indication of an increasing frequency of occurrence of the emitter at all locations. Because of some instrumental uncertainties, it is not possible to be certain that this effect is real and not instrumental.

To study the relationships of the emitter to other meteorological parameters, the emitter distributions were compared with the mean potential temperature, mean temperature, and mean vertical temperature gradients which existed at the time of the observations. These results are presented in Figures 9 through 11.

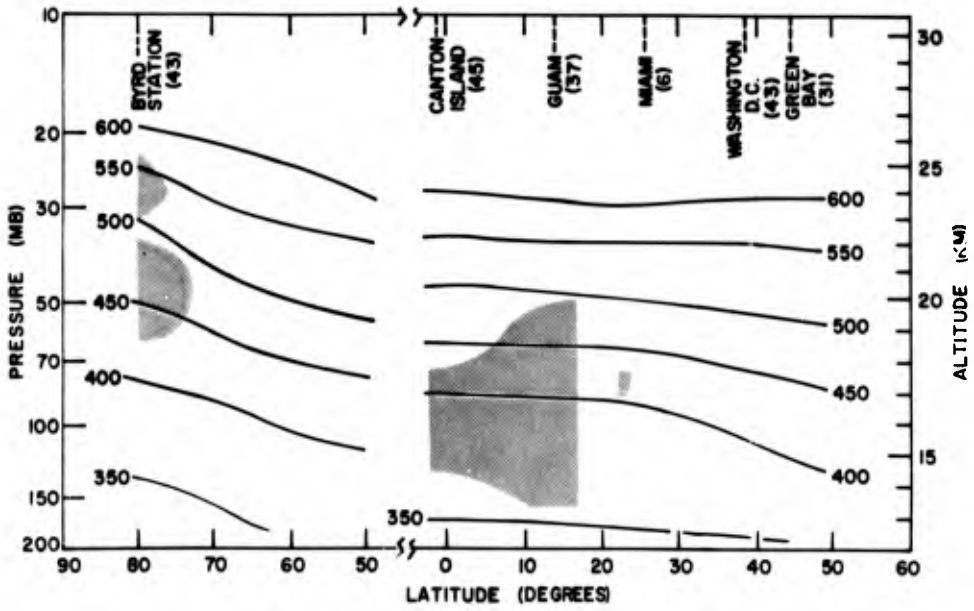

Figure 9. Latitudinal Cross-Section of the Mean Potential Temperature Field for April 1964-December 1965 Period.

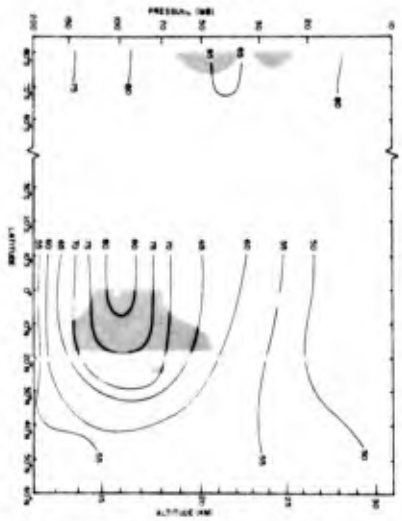

Figure 10. Latitudinal Cross-Section of the Mean Temperature (°C) Field During the April 1964-December 1965 Period.

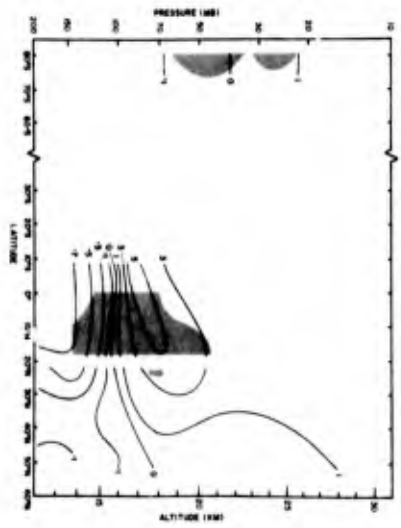

Figure 11. Latitudinal Cross-Section of the Mean Temperature Lapse-Rate (°C/km) Field During the April 1964-December 1965 Period.

It is not possible to say, on the basis of these annual means, that the greatest concentration of the emitter is always found along preferred potential temperature surfaces. Maximum concentrations in the tropics appear to be in the region between $\theta = 375°K$ and $\theta = 425°K$. In the mid-latitudes, the β_{abs} values peak in the same region with θ about 400°K. The frequency of occurrence isopleths cut across the isentropes in several instances and these two fields show no relationship to each other. In Antarctica, however, both the frequency of occurrence and the concentration have a maximum in the vicinity of the 450°K isentrope.

A significant relationship is noted between the temperature field and the emitter distribution. The greatest emitter concentrations are most likely to occur at low temperatures and in the region of temperature inversions. Almost all areas of large β_{abs} are at temperatures below minus 65°C. The values dT/dz associated with the greatest concentrations are typically +1° to +3°C/km or greater. A notable exception to this exists in Antarctica, where there are significant concentrations of the emitter at altitudes where no inversions are present.

More detailed vertical profiles of the β_{abs}, frequency of occurrence, temperature gradient are presented in later sections which deal with the various geographic regions in greater detail.

Relationship of Emitter to Stratospheric Circulation.

It is interesting to speculate what circulation patterns must exist in the lower stratosphere to account for the mean emitter distributions shown in Figure 7.

Based on an analysis of stratospheric aerosol particles obtained in-situ by samplers, Junge [23] and others have concluded that this aerosol contains large concentrations of sulphates. Various schemes explaining how this can come about have been discussed, but a recent theory by Scott and Lamb [49] appears to be most consistent with our observations of the aerosol. Their explanation is as follows: gases SO_2 and NH_3 are pushed through the tropical tropopause by a slow upward vertical motion. Reactions begin to occur in the lower tropical stratosphere: a direct reaction between SO_2 and NH_3 takes place at the extremely cold tropical tropopause temperatures to produce sub-micron-sized solid particles. These particles are then oxidized and hydrolized to form sulfates. At the same time, at slightly higher altitudes, some of the remaining SO_2 reacts with atomic oxygen to form SO_3 which reacts readily with ammonia to form ammonium sulfate by hydrolysis. Scott and Lamb further postulate that these particles then diffuse to higher latitudes, coagulating to form the larger particles observed by optical and impactor techniques.

The global distributions of the aerosol obtained from the radiometersonde tend to support this theory. First, the fact that we observe with the radiometersonde a greater mass of the aerosol than LIDAR techniques, especially in the tropics, would confirm the presence of small particles which are still undergoing a growth process, both by coagulation and by hygroscopic action. Because of the greater measured concentration in the tropics, the source of much of the stratospheric aerosol may be in this region.

An examination of Vincent's [53] analysis of the stratospheric circulation for the 1964-1965 period, presented in Figure 12, indicates that the upward vertical motions necessary for the formation of the aerosol existed at latitudes south of 30°N. A mean poleward motion in the 100 mb-30 mb region is present between 20° and 40° latitude accounting for the poleward transport of the aerosol. The situation becomes more variable with the seasons at latitudes greater than 40°, but the area between 40° and 60° latitude shows generally downward vertical motion and little horizontal transport.

Thus, it is possible that the aerosol formed over the tropics would be transported poleward in irregular impulses, dependent on the seasons and the synoptic circulation patterns. As this aerosol is moved poleward along the isentropes, adiabatic heating of the air would take place, resulting in warmer temperatures. This, in turn, would cause the evaporation of some of the volatile aerosol. However, as the material is advected further poleward and adiabatic cooling takes place, the gases may again recondense and form particulates.

Tropical Measurements.

a. Mean Profiles. The mean vertical profiles of β_{abs}, temperature, lapse rate and of the frequency of occurrence of the aerosol are considered first. From Figures 13a and 13b we see that even though the temperature and stability profiles for Guam and Canton Island are almost identical, some significant

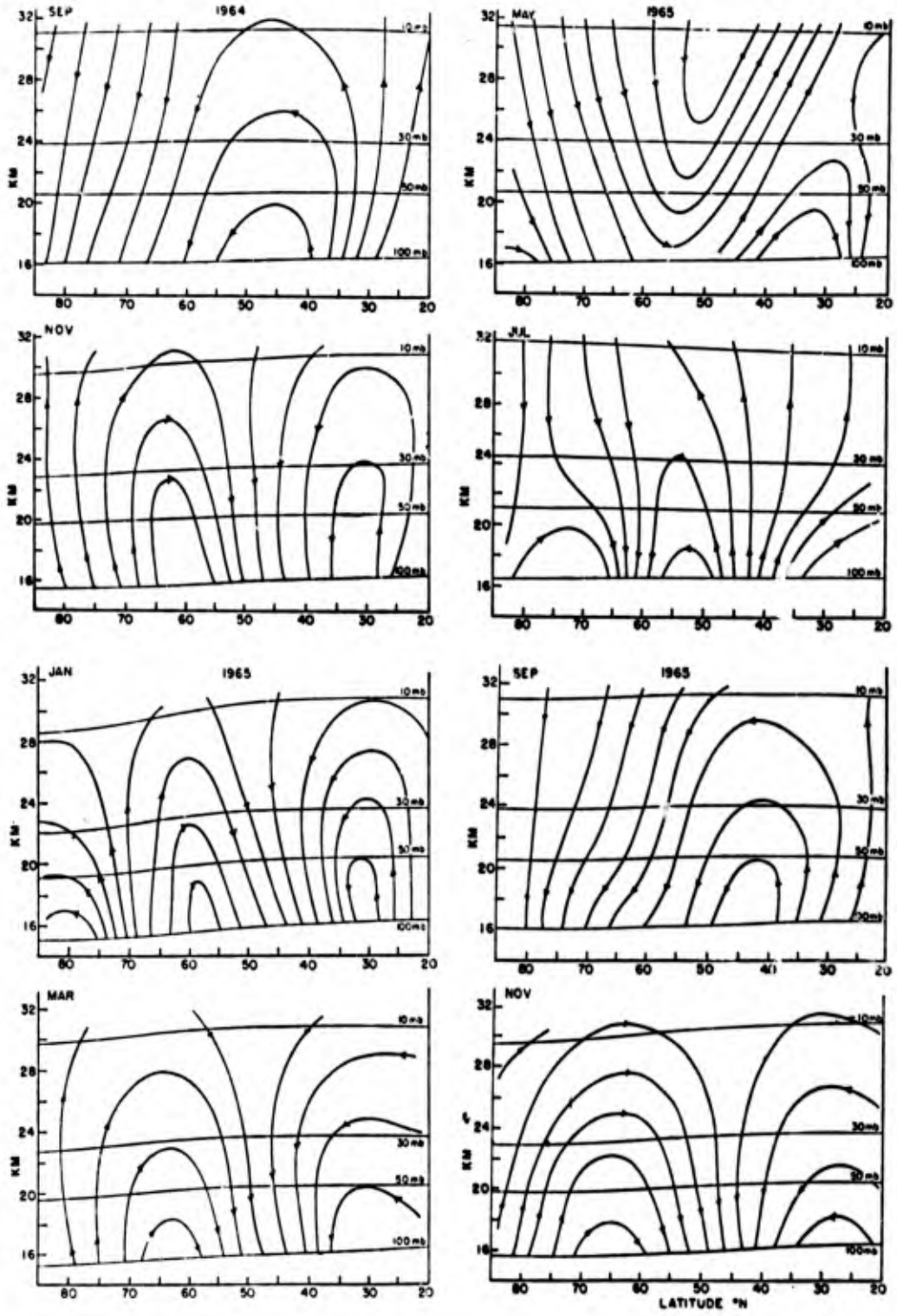

Figure 12. Flow Patterns for Meridional Circulations for the September 1964-November 1965 Period (from Vincent [53]).

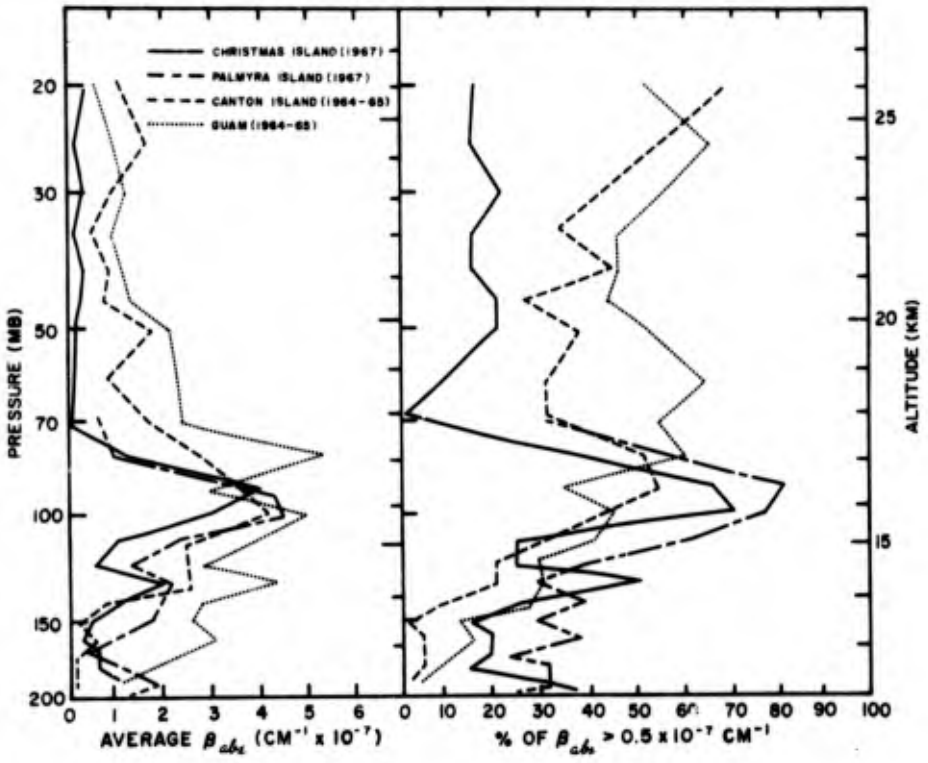

Figure 13a. Mean Tropical Profiles — Absorption Coefficient and Frequency of Occurrence of Emitters.

differences in the aerosol profiles are present. Canton Island has a well-defined maximum of occurrences between 120 and 70 mb, with a maximum of 55% at 90 mb. There is a flat minimum between 70 and 35 mb with increasing frequencies above that level. Guam has more frequent occurrences of emitter at most levels, with a maximum of 65% at 60 mb and again at 25 mb.

The profiles of the mean concentration show that Canton Island has a maximum $\beta_{abs} = 4 \times 10^{-7} cm^{-1}$ at 100 mb, and a small secondary maximum at 50 mb. Guam shows a more layered structure, with one maximum of $5.3 \times 10^{-7} cm^{-1}$ at 80 mb, and another at 100 mb with $\beta_{abs} = 5.0 \times 10^{-7} cm^{-1}$.

The mean profiles for the Line Island data from Christmas Island and Palmyra Island are also displayed in Figures 13a and 13b. It should be noted that while the Guam and Canton Island data represent mean values for a year from mid-1964 to mid-1965, the Line Island data were obtained in a one-month period in early 1967.

The profiles for the Line Island data are quite similar and resemble Canton Island more than Guam. Most notable are the very high frequency of occurrence in the 90-70 mb region (70% to 80%), and a value for β_{abs} of about $5 \times 10^{-7} cm^{-1}$ at the same altitude. It is also noteworthy that not one of the 20 profiles taken at Christmas Island showed the presence of any aerosol at the 70-mb level during the 30-day observation period. The 70-mb region in the Canton Island time series also seems to be a region of low emitter concentrations.

The Canton Island and Line Island profiles indicate a maximum occurrence and concentration of the emitter just above the tropical tropopause. Guam, on the other hand, shows the most frequent and greatest concentrations about 1 to 3 km above the tropopause. The great concentrations of β_{abs} at altitudes below 140 mb at Guam are probably due to tropical storm activity.

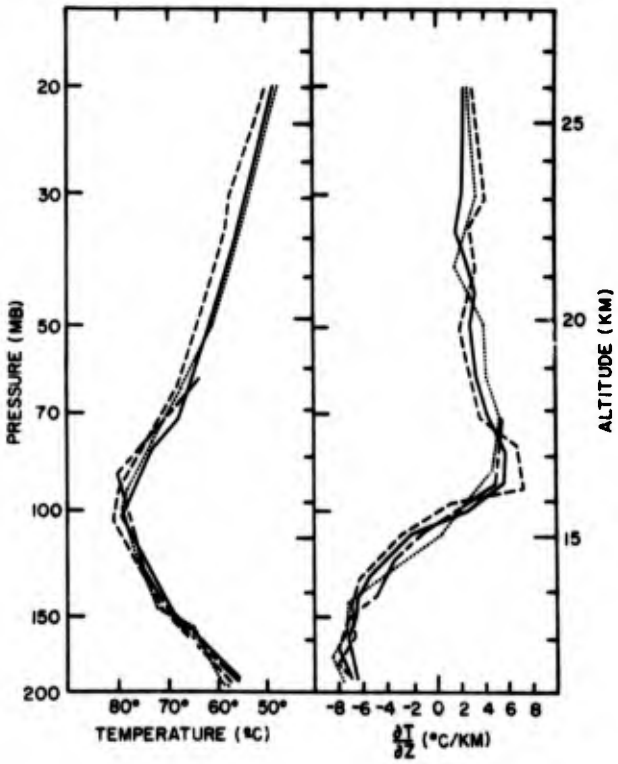

Figure 13b. Mean Tropical Profiles — Temperature and Temperature Lapse Rate (refer to Figure 13a for Key).

The strongly-diminished values of both concentration and frequency of occurrence for Christmas Island at altitudes above 60 mb may indicate that the stratospheric emitter at these altitudes had significantly diminished in the two years since the Guam and Canton Island data had been obtained. This may well be related to the fallout and diffusion of the aerosol injected into the atmosphere by the Agung eruption of March 1963. If this is the case, then the data for the 1964-1965 period may represent a condition of enormously high aerosol concentrations.

b. Monthly Time Series. Monthly time cross-sections of β_{abs}, temperature, lapse rate, and frequency of occurrence for the 1964-1965 time period are presented for Guam in Figure 14a through Figure 14d; for Canton Island in Figure 15a through Figure 15d. We note the presence of a well-defined layer over Canton Island between 120 mb and 90 mb, and another layer of lower concentrations in the vicinity of 25 mb. A pronounced minimum exists over this location from about 40 to 30 mb. There also appear to be injections of aerosol from the 90-mb region into higher altitudes at periodic intervals. These injections appear only in the monthly means, however, and cannot be traced on the individual sounding profiles. Thus, there is some question as to whether they are real.

It is also apparent that Guam is occasionally affected by cirrus from tropical storms, as the increased values of β_{abs} at altitudes below 120 mb in October-November 1964 and September 1965 indicate. No other influences of tropical-storm activity on the radiometersonde data were noted.

It is desirable to compare the vertical motion field with the vertical

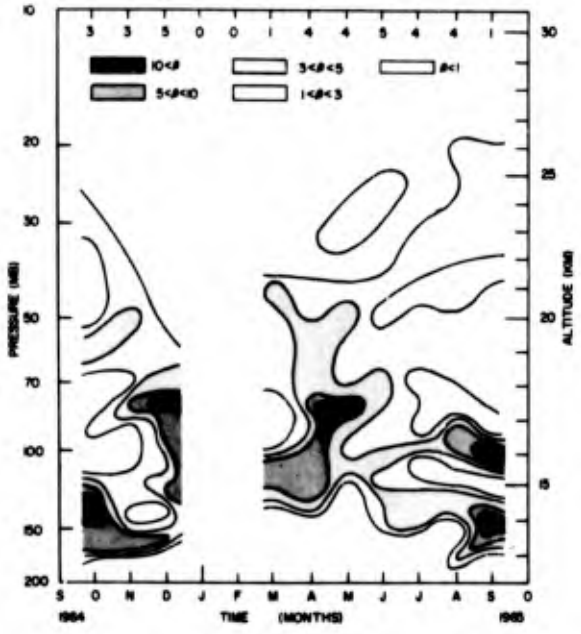

Figure 14a. Guam Monthly Time Series — Absorption Coefficient ($\beta_{abs} \times 10^{-7} cm^{-1}$).

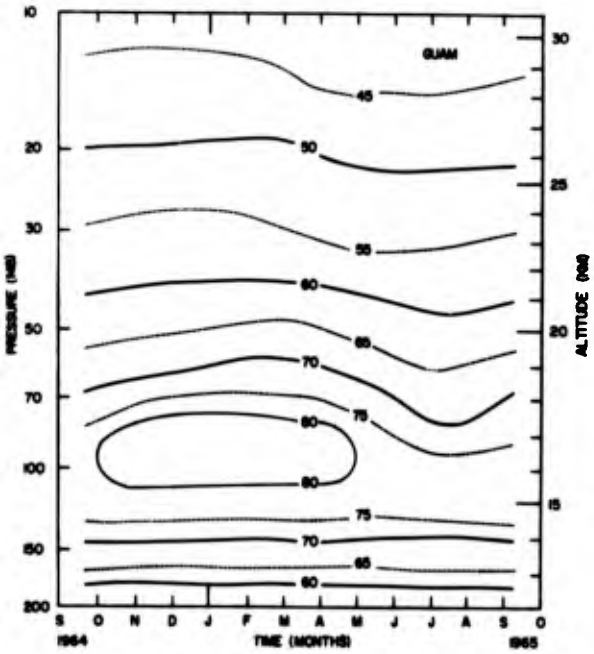

Figure 14c. Guam Monthly Time Series — Temperature (°C).

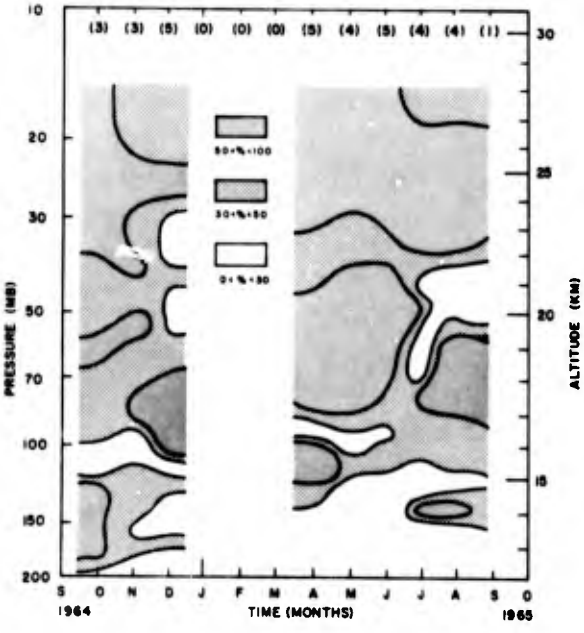

Figure 14b. Guam Monthly Time Series — Percent Frequency of Occurrence of Emitters.

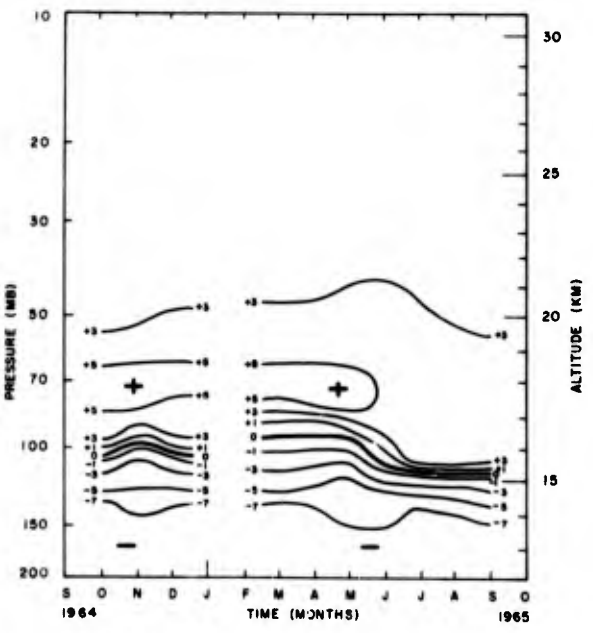

Figure 14d. Guam Monthly Time Series — Temperature Lapse Rates (°C/km).

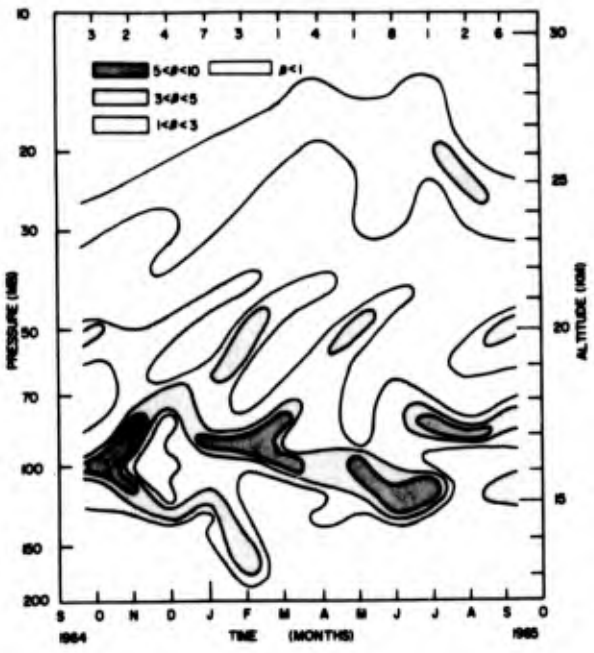

Figure 15a. Canton Island Monthly Time Series — Absorption Coefficient ($\beta_{abs} \times 10^{-7} cm^{-1}$).

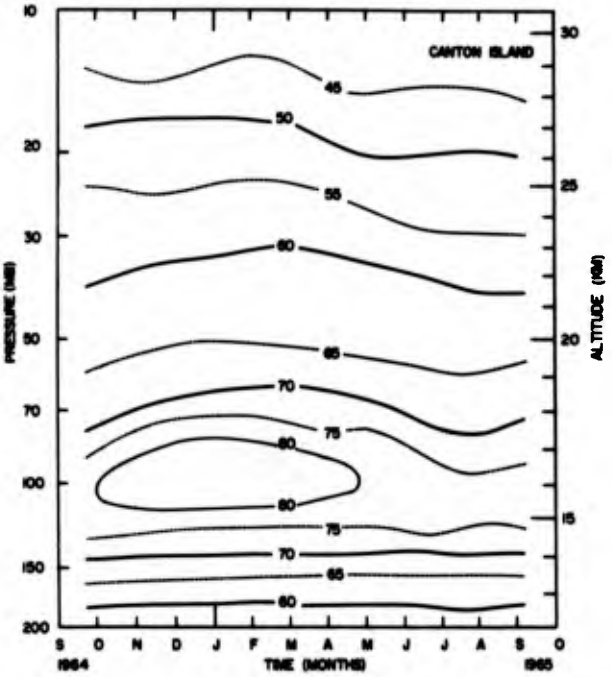

Figure 15c. Canton Island Monthly Time Series — Temperature (°C).

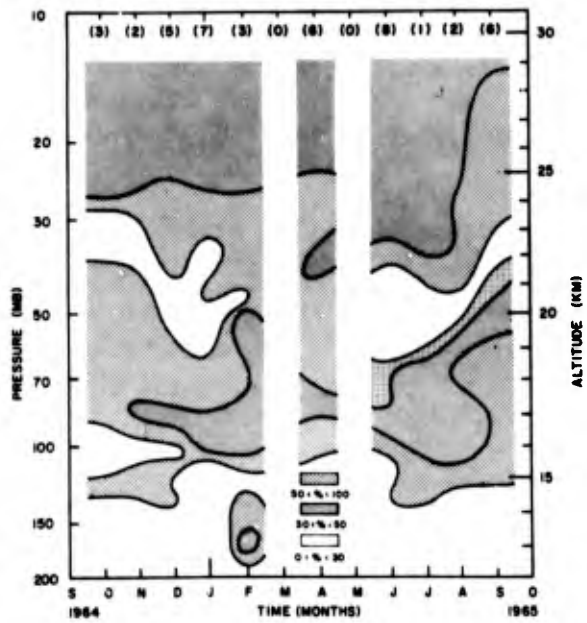

Figure 15b. Canton Island Monthly Time Series — Percent Frequency of Occurrence of Emitters.

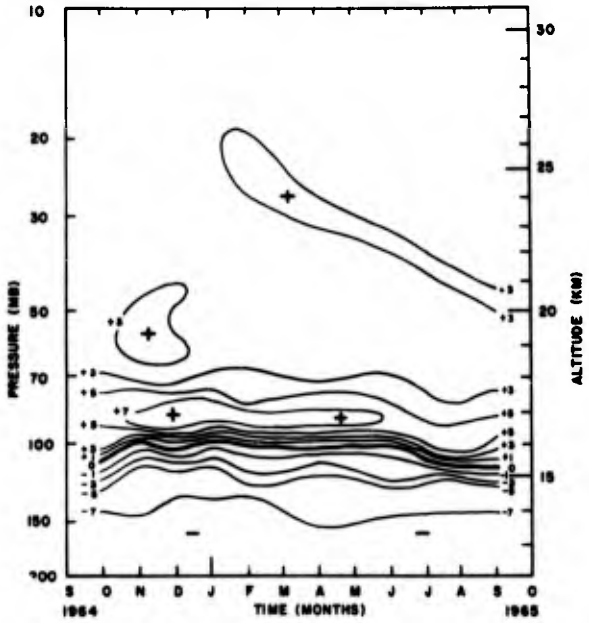

Figure 15d. Canton Island Monthly Time Series — Temperature Lapse Rate (°C/km).

emitter profiles. The vertical motion data were not available for the 1964-1965 period for the tropics. However, a time series based on 1957-1958 data is available. Figure 16 shows the three-monthly mean adiabatic vertical motions at the 75-mb level, as calculated by Miller [37] for Guam, Green Bay, and Washington. From September through March, downward vertical motions predominate over Guam. From March through August, the vertical motion there is predominately upward. Despite the lack of emitter data for the January-February period, we see that the vertical motion field and the mean monthly β_{abs} values at Guam seem to be related. Especially noteworthy is the increased emitter concentration in the 50 mb-70 mb region during the April-May period, a time when the upward vertical motion is probably at its maximum.

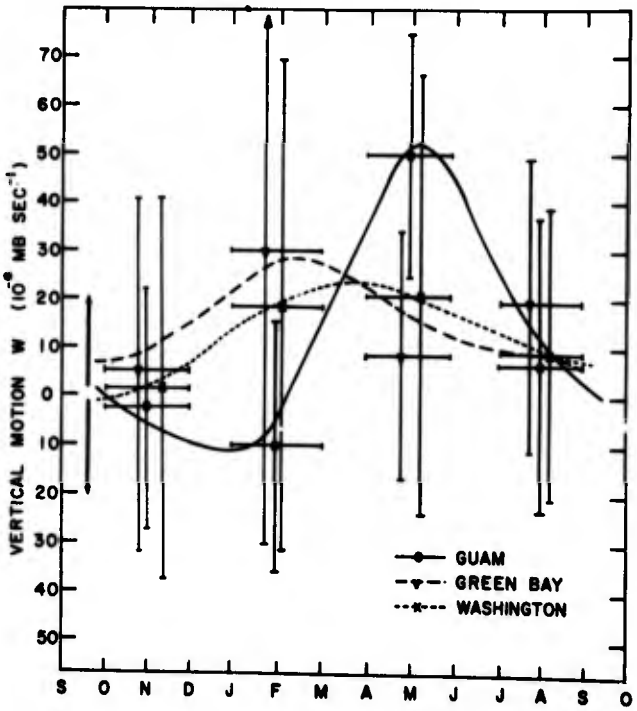

Figure 16. Vertical Motions at 75 mb for Guam, Green Bay, and Washington during 1958-1959 (from Miller [37]).

No vertical motion data from Canton Island were available. However, an examination of Miller's data indicates that at the equator about 172°W the vertical motion at 75 mb was essentially zero over the entire year, with a small value of standard deviations for the same period. This does not agree with our radiometersonde data for Canton Island, which show a periodic variation in the mean monthly β_{abs} values at this altitude.

c. Daily Time Series. During the Line Island experiment a number of radiometersonde ascents were made on an almost daily basis from 22 March to 23 April 1967. Twenty ascents from Christmas Island and 21 flights from Palmyra were found suitable for analysis. The Palmyra data, it should be noted, terminated at 60 mb. In addition, the existence of data gaps of several days duration at both locations made this a less than perfect time series. Despite such shortcomings, these data form our best record of the day-to-day variations of the stratospheric aerosol over the tropical Pacific. The time series of β_{abs} is presented in Figure 17 for Christmas Island and in Figure 18 for Palmyra. Wind data from the stations are in Figures D-3 and D-6, respectively. Time series of various other meteorological parameters, such as temperature and lapse rate, can also be found in Appendix D.

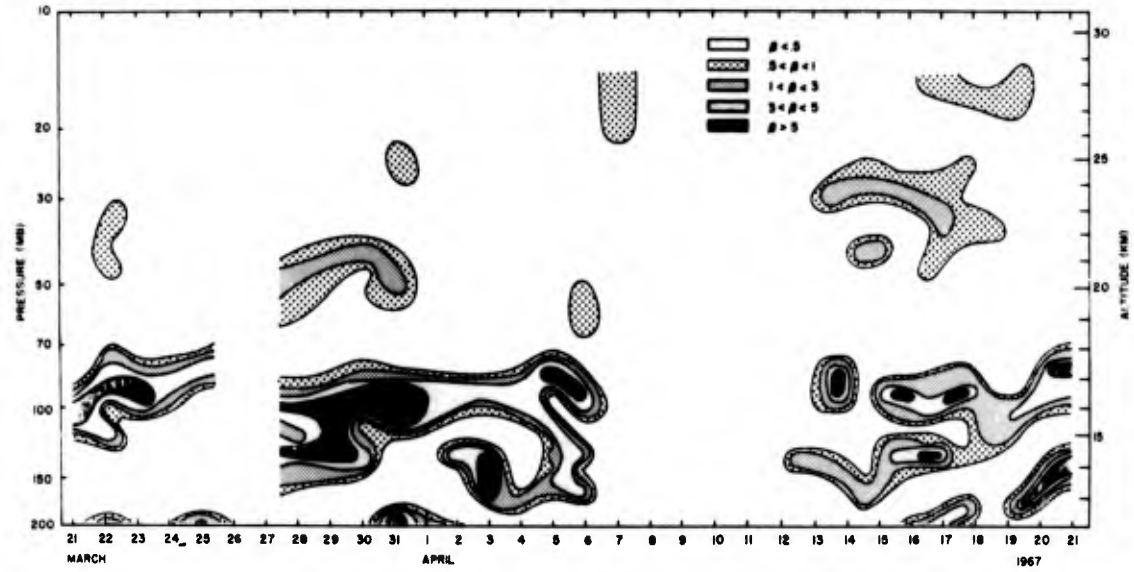

Figure 17. Christmas Island Daily Time Series — Absorption Coefficient ($\beta_{abs} \times 10^{-7} cm^{-1}$).

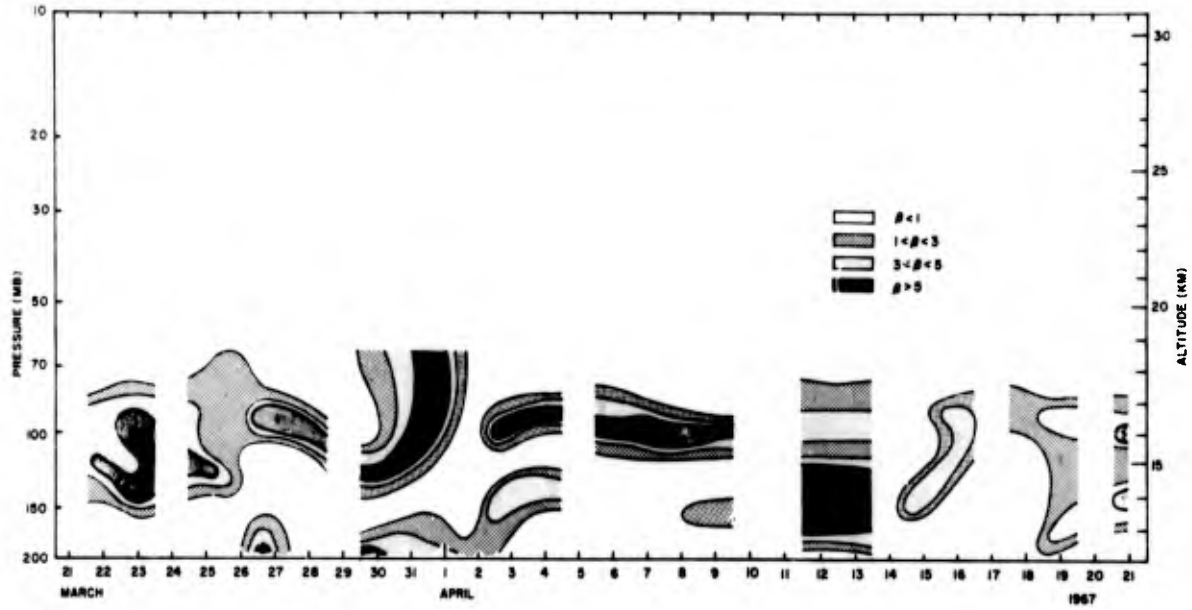

Figure 18. Palmyra Island Daily Time Series — Absorption Coefficient ($\beta_{abs} \times 10^{-7} cm^{-1}$).

The β_{abs} time series for both locations appear to be similar, but no obvious relationship between the two series was evident. A possible exception to this is the period 1-3 April, when a tropical disturbance was in the area and apparently injected some cirrus into the lower stratosphere which is evident at both locations. While most of the aerosol layers persist from day to day, others appear and disappear from one day to another. In Appendix D Figures D-3 and D-6 indicate that the emitter is concentrated in the layer of greatest wind shear which, in this case, also corresponds to the region just above the tropopause.

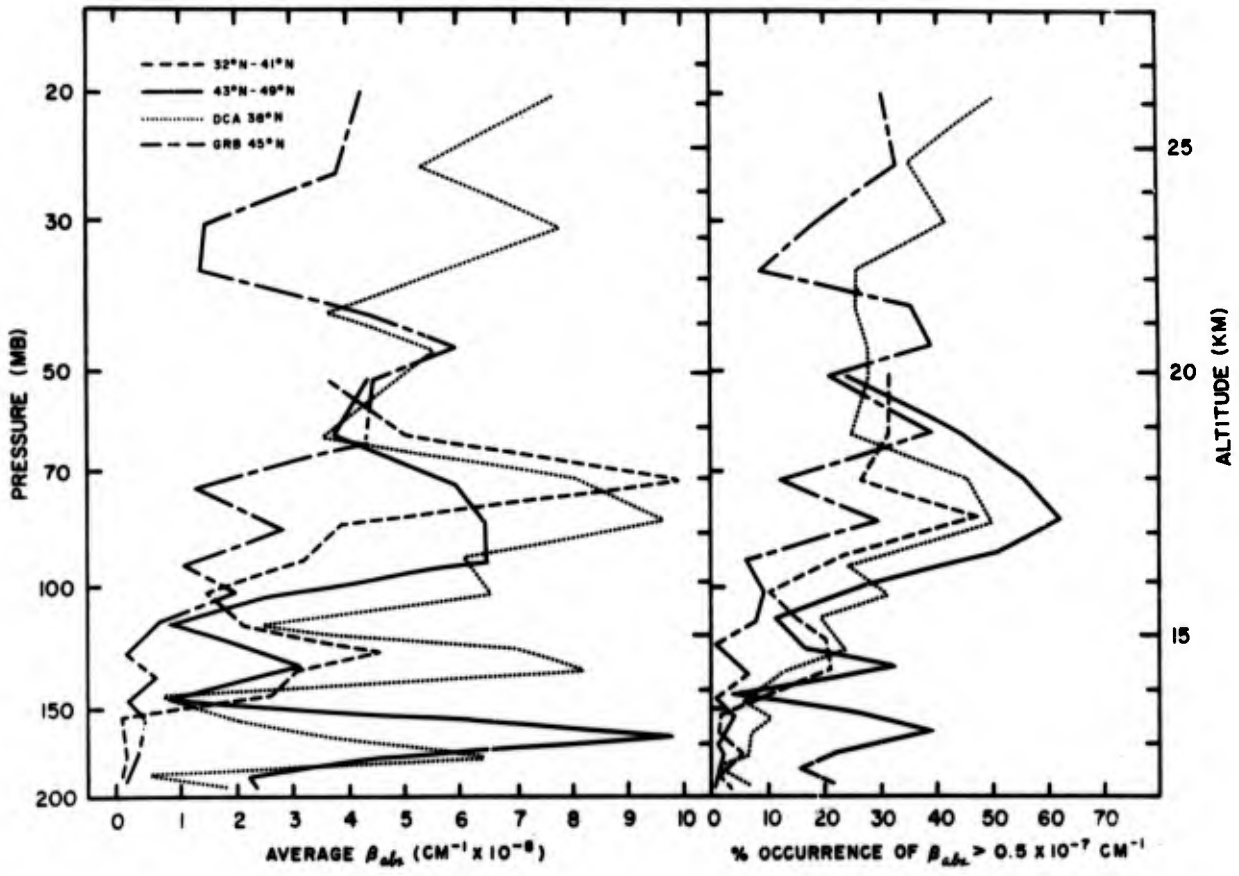

Figure 19a. Mean Temperate Latitude Profiles — Absorption Coefficient and Frequency of Occurrence of Emitters.

Temperate-Zone Measurements.

a. Mean Profiles. It is obvious from Figures 19a and 19b that while the mean temperature and thermal stability patterns for Green Bay and Washington are almost identical, the mean aerosol profiles show significant differences. The pronounced peak in the frequency of occurrence curve for Washington shows that the aerosol here is most likely to exist between 90 and 60 mb, with another small maximum at 30 mb. The average concentration profile has a similar shape, with the greatest value of $\beta_{abs} = 1 \times 10^{-7} cm^{-1}$ at 80 mb. The aerosol structure over Green Bay, on the other hand, has several sharp maxima in the frequency of occurrence, and at altitudes below 50 mb, these values are only one-third of what they are at Washington. The values for β_{abs} at Green Bay were found to be about one-third of what they are in Washington at altitudes below 50 mb. The greatest concentrations over Green Bay are at altitudes between 80 and 35 mb with the maximum $\beta_{abs} = 0.6 \times 10^{-7} cm^{-1}$ at 45 mb.

Since the Green Bay data are heavily biased with January observations, such a disagreement should not be unexpected, and the location of the maximum emitter

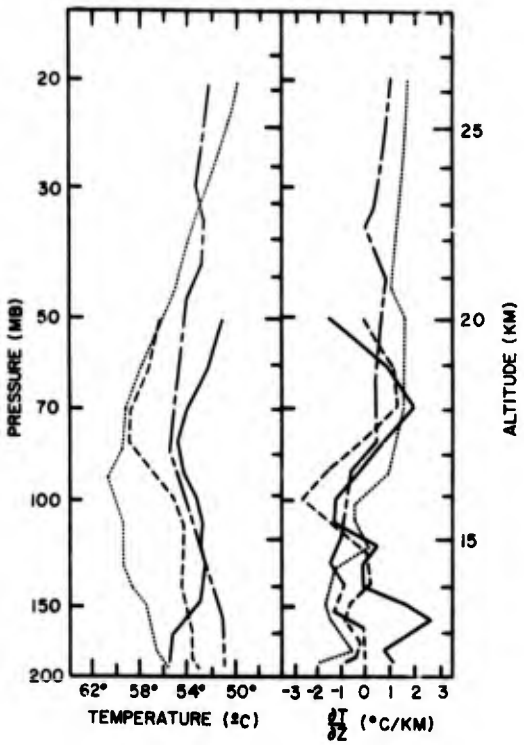

Figure 19b. Mean Temperate Latitude Profiles — Temperature and Temperature Lapse Rate (refer to Figure 19a for key).

concentrations at the high altitudes actually agrees well with Antarctic winter data.

The mean profiles of the radiometersonde ascents made over the Central United States on 12 December 1965 are also displayed in Figures 19a and 19b. Profiles of β_{abs} and frequency of occurrence for both the northern and southern sections of this area show a strong similarity to the Washington profiles. The very high concentration observed over the northern area at about 170-mb altitude is probably due to the influx of cirrus cloudiness from an intense storm system centered over Wisconsin at that time.

b. Monthly Times Series. Sufficient data are not available to present a monthly time series of the mean profiles for an entire year at a mid-latitude site, as Washington and Green Bay both have periods of observation shorter than one year. The data are displayed in Figures 20a through 20d and Figures 21a through 21d. The most obvious difference between these monthly times series and those in the tropics is that the concentration of aerosols in the tropics in the region between 100 and 70 mb is almost a factor of five greater than in the mid-latitudes. This seems to be true at any time of year.

None of the two mid-latitude distributions shows any meaningful seasonal trends, except for increased concentrations at Green Bay and Washington in November, followed by a pronounced minimum in January. Washington shows increased concentrations again during the May-June period; no data from Green Bay for this period are available. For the whole year, the most persistent feature is a layer of moderate concentration at 90 to 70 mb over Washington.

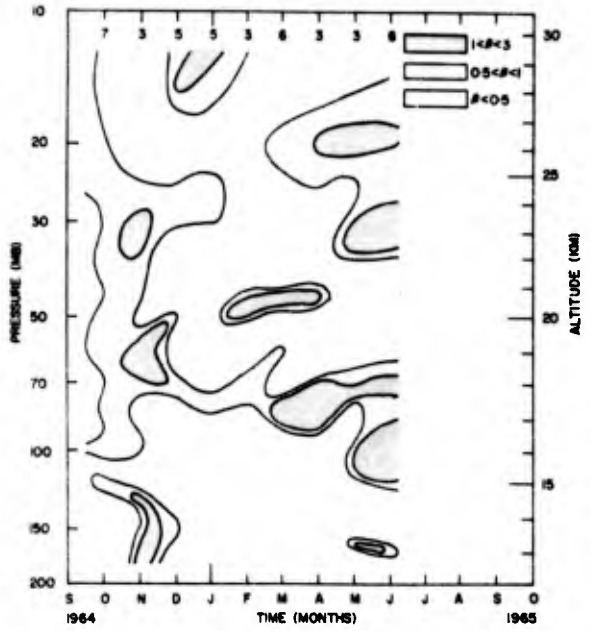

Figure 20a. Washington Monthly Time Series — Absorption Coefficient ($\beta_{abs} \times 10^{-7} cm^{-1}$).

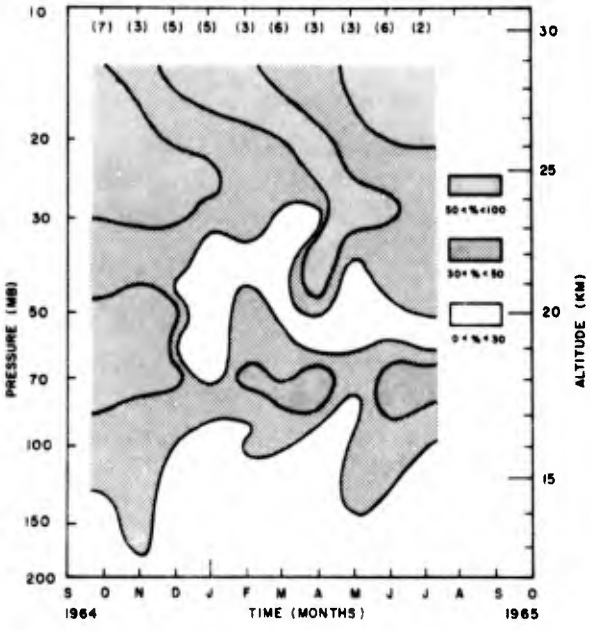

Figure 20b. Washington Monthly Time Series — Percent Frequency of Occurrence of Emitters.

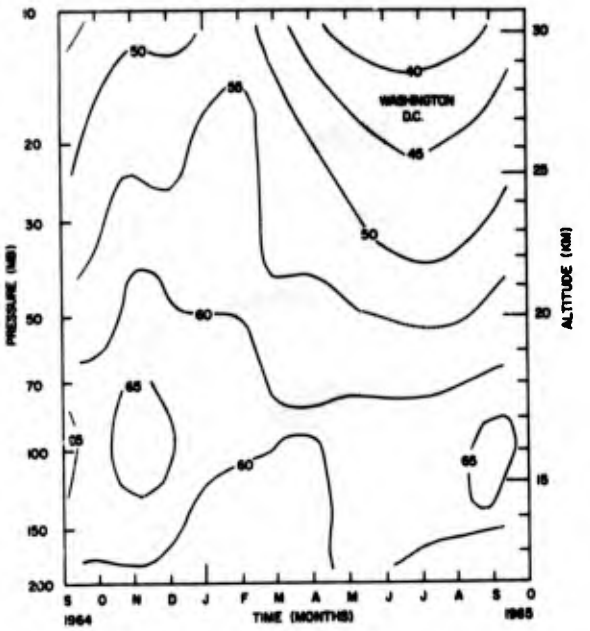

Figure 20c. Washington Monthly Time Series — Temperature (°C).

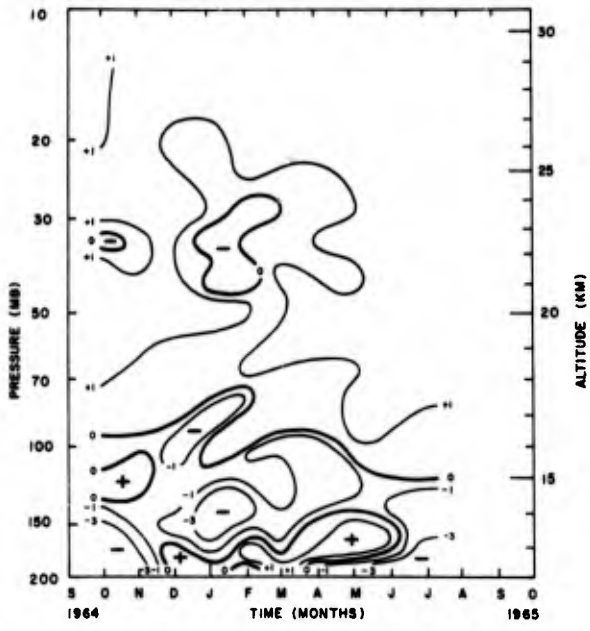

Figure 20d. Washington Monthly Time Series — Temperature Lapse Rate (°C/km).

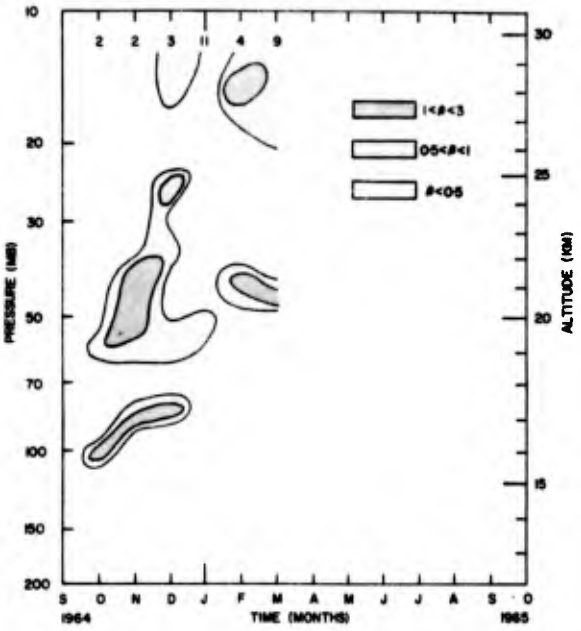

Figure 21a. Green Bay Monthly Time Series — Absorption Coefficient ($\beta_{abs} \times 10^{-7} cm^{-1}$).

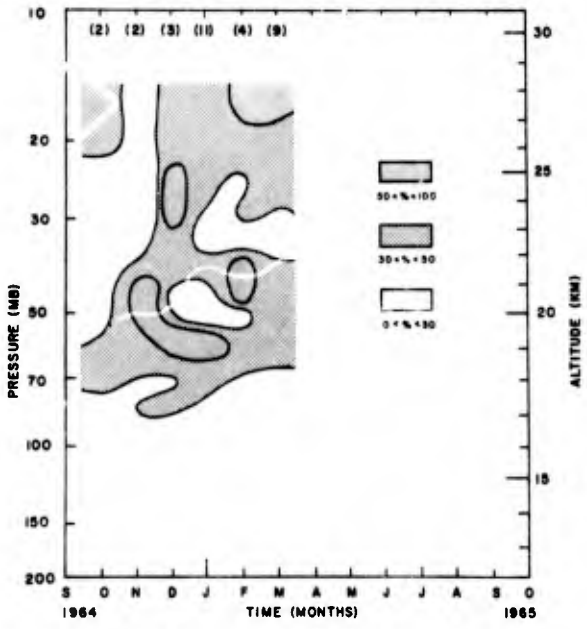

Figure 21b. Green Bay Monthly Time Series — Percent Frequency of Occurrence of Emitters.

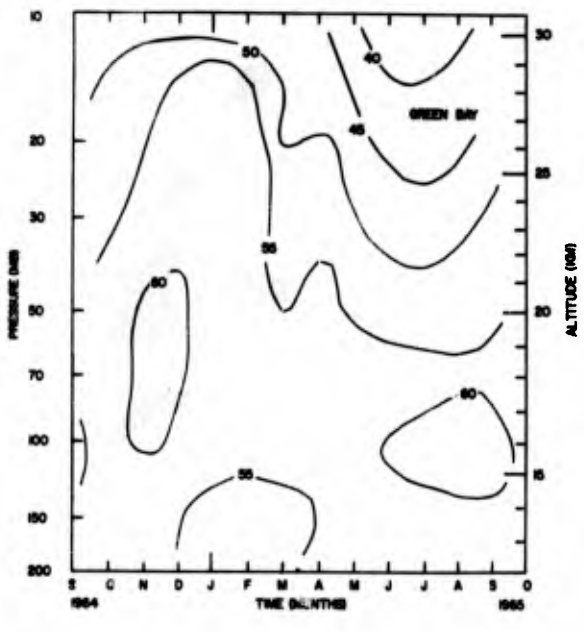

Figure 21c. Green Bay Monthly Time Series — Temperature (°C).

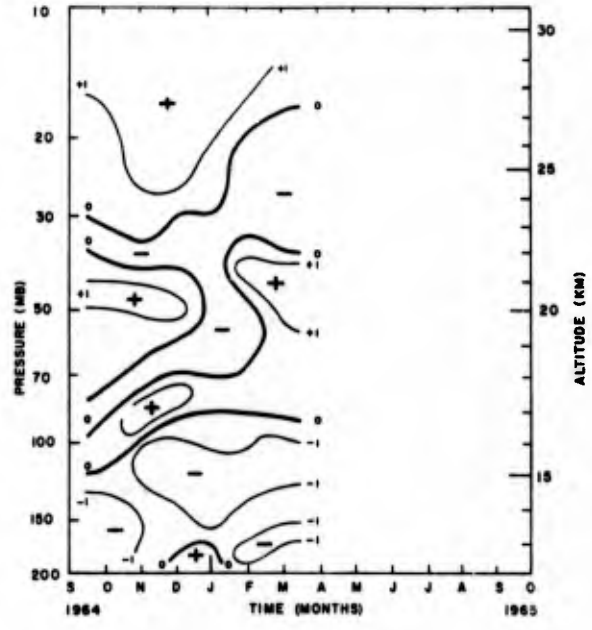

Figure 21d. Green Bay Monthly Time Series — Temperature Lapse Rate (°C/km).

It is interesting to compare our results with those obtained by Grams and Fiocco [19]. Whereas the infrared analysis indicates no significant change in the mean monthly concentrations at Washington from September 1964 to July 1965, the LIDAR data from the Boston area (see Figure 22) indicate a significant annual variation of the aerosol over the September 1964-September 1965 period, superimposed on an overall trend toward decreasing concentrations. A possible explanation is that with the radiometersonde we are looking at an aerosol which has a different origin than the predominately volcanic-origin aerosol which was so much in evidence at that time (Volz [55]). It should be noted that the sampling statistics of the radiometersonde are poorer than those of the LIDAR, and the poor agreement may be due to this fact.

Looking again at Figure 16 we see that over Green Bay the prevailing vertical motion through the 75-mb level is upward for the period that the aerosol data are available. This is also true for Washington. As pointed out earlier, however, there is some doubt as to whether Miller's 1957-1958 results can be applied to the 1964-1965 time period. An attempt to determine a relationship between the aerosol distribution and Vincent's [53] analysis of the stratospheric circulation is perhaps more meaningful. The circulation data in Figures 23 and 24 are based on Vincent's results and the regions of maximum aerosol concentrations are stipled in. Regrettably, Vincent's results are only for altitudes above 100 mb. Nevertheless, we see that the enhanced aerosol concentrations reported by Grams are present when the mean flow is southward and the mean vertical motion is downward. This suggests that the winter polar region may be an aerosol reservoir. On the other hand, the aerosols which appear in the autumn may be of tropical origin.

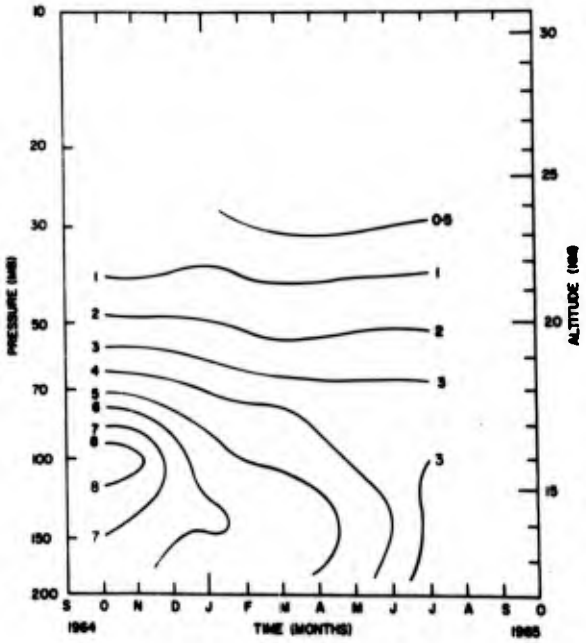

Figure 22. Monthly Time Series for LIDAR Backscatter Coefficient ($\times 10^{-10}$ cm^{-1} sr^{-1}) over Boston for September 1964-July 1965 (from Grams and Fiocco [19]).

c. Synoptic Scale Analysis. No extended time series of daily radiometersonde data in the mid-latitudes is available. On 12 December 1965, however, a unique synoptic-scale experiment was conducted to measure the radiation field of a low-pressure system over the midwestern United States (Cox [7]). Several dozen radiometersondes were launched from a number of locations from Alabama to Minnesota, with as many as five ascents being made from one location during a

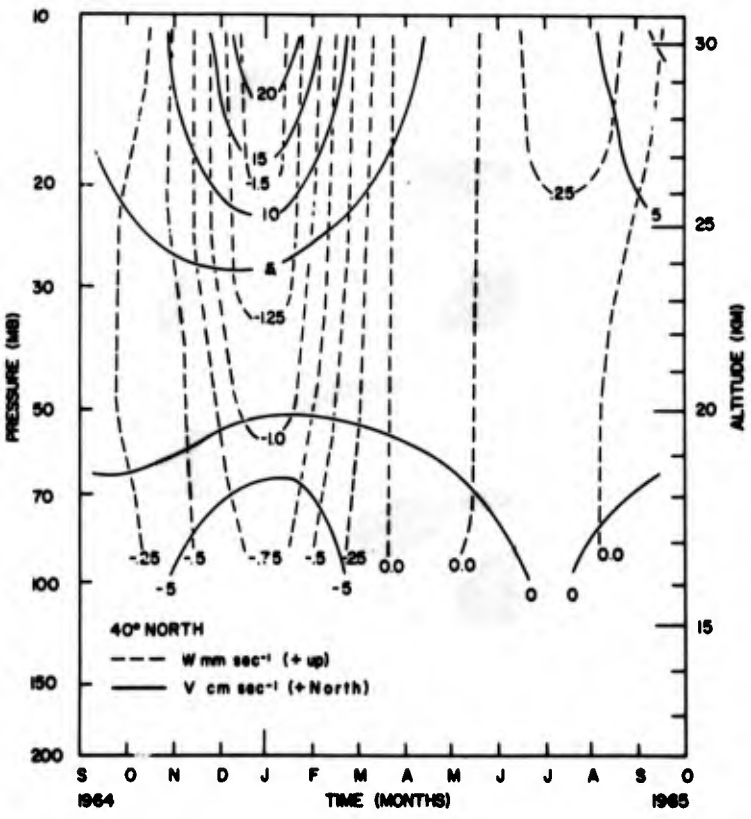

Figure 23. Monthly Time Series for Vertical and Meridional Motion Fields at 40°N for September 1964-September 1965.

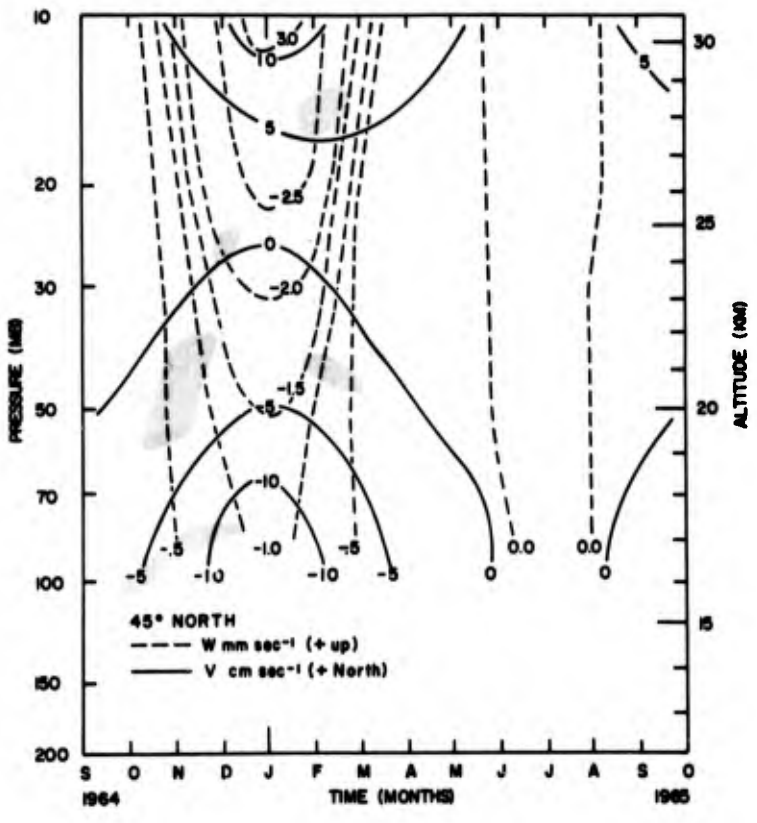

Figure 24. Monthly Time Series for Vertical and Meridional Motion Fields at 45°N for September 1964-September 1965.

12-hour period. Thirty-seven of these flights reached the 50-mb level and were analyzed for aerosol concentration.

Mean profiles for the northern and southern group of ascents are presented in Figures 19a and 19b. This analysis of the 12 December 1965 data indicates that in the region from 70 to 90 mb, the altitude of maximum β_{abs}, emitter concentrations in excess of the sensitivity limit of the radiometersonde ($\beta_{abs} \simeq 0.5 \times 10^{-7} cm^{-1}$ at this altitude) were observed in about 50% of the soundings. The mean values of β_{abs} were $0.8 \pm 0.2 \times 10^{-7} cm^{-1}$, while individual values ranged from zero to more than $5 \times 10^{-7} cm^{-1}$.

An examination of data for various locations which had several ascents during a 12-hour period (see Figure 25) leads to the conclusion that the emitter detected by the radiometer is a highly variable phenomenon. Considering the wind speeds at these altitudes, it may be possible to speculate that the emitter clouds, in some cases, are less than 50 miles in size or, at least, have some discontinuities on this scale, while others persist for most of the 12-hour period implying a horizontally homogeneous extent of hundreds of miles.

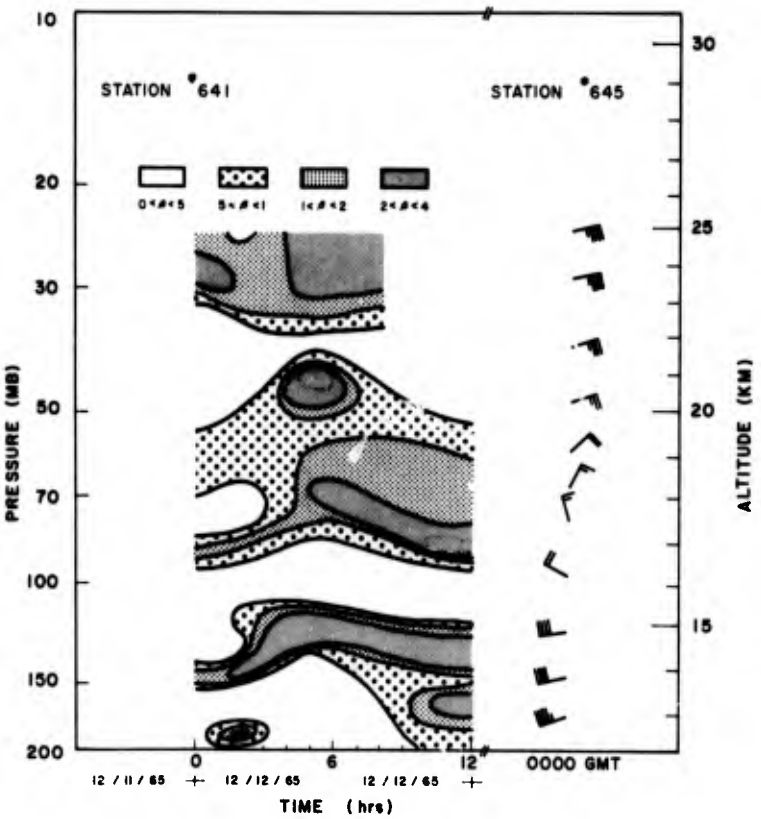

Figure 25. Madison Three-Hourly Time Series of Absorption Coefficient ($\beta_{abs} \times 10^{-7} cm^{-1}$) on 12 December 1965.

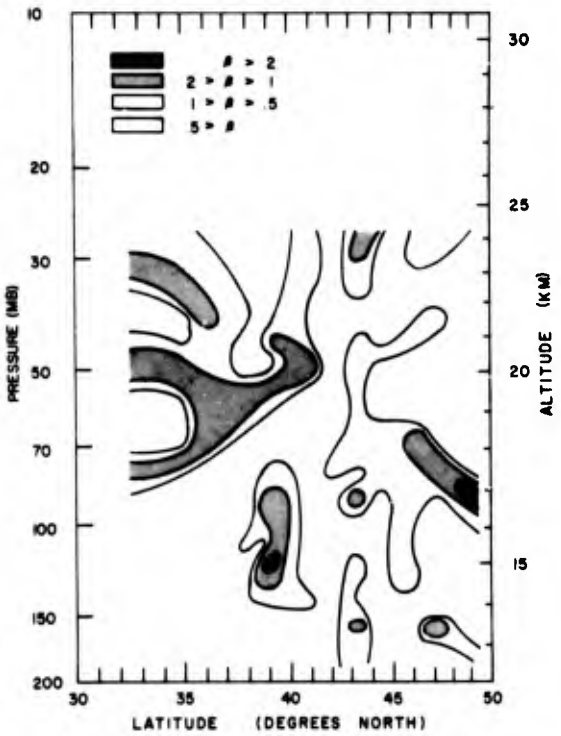

Figure 26a. Central United States Latitudinal Cross-Section of the Absorption Coefficient ($\beta_{abs} \times 10^{-7} cm^{-1}$) on 12 December 1965.

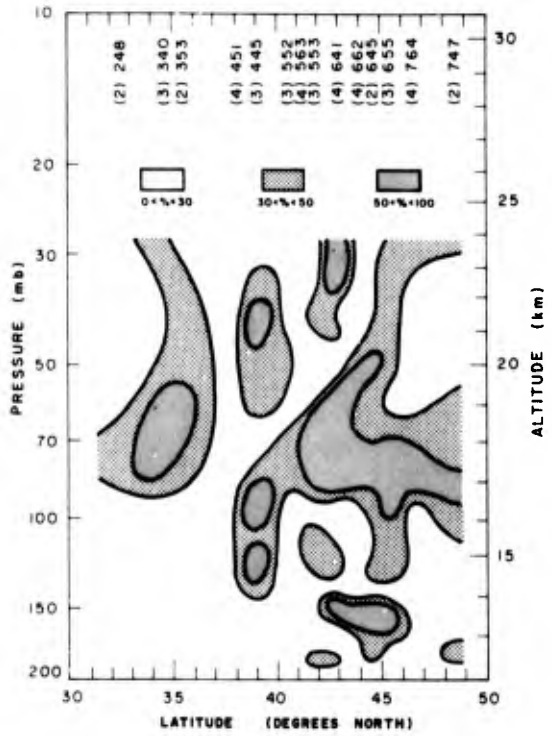

Figure 26b. Central United States Latitudinal Cross-Section of the Percent Frequency of Occurrence of Emitters on 12 December 1965.

This analysis leads to the conclusion that this emitter, rather than being a more or less permanent feature of the stratosphere, as may have been implied by some investigators, is actually more analogous to cirrus cloudiness. It does have certain preferred levels of occurrence, but apparently makes an appearance only under certain synoptic conditions which are not apparent when only mean monthly or seasonal circulations are considered.

A longitudinal cross-section of the average β_{abs} at each observing location is presented in Figure 26a. There is no uniform layer such as we may expect to see at the 80-mb level, but rather a disorganized grouping of emitters which does not seem to correlate with any of the meteorological parameters measured. An investigation of the frequency of occurrence of the emitter along the same cross-section in Figure 26b shows that there does not appear to be any obvious relationship to conventional meteorological parameters, except possibly to the temperature lapse rate. Not surprisingly, we find the emitter occurring most frequently in the region of greatest stability.

An analysis of the frequency of occurrence of the emitter in the layer between 70 and 90 mb on 12 December 1965 is presented in Figure 27. There appear

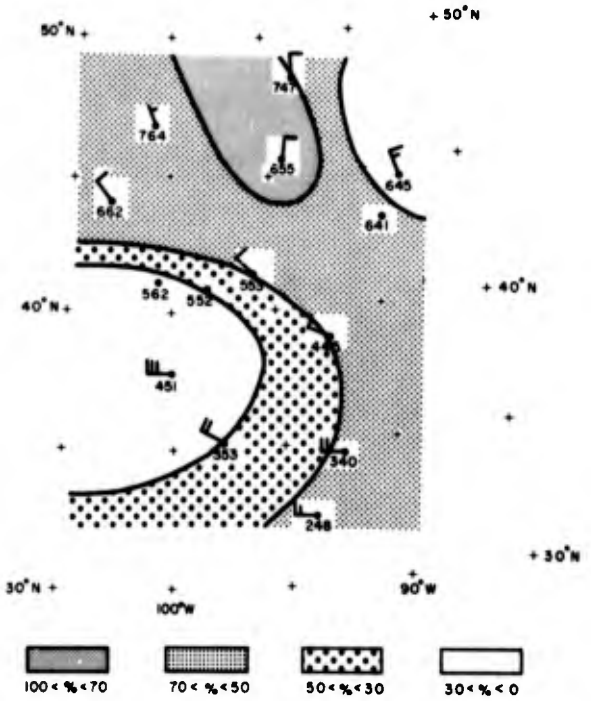

Figure 27. Percent Frequency of Occurrence of Emitters Between 70 mb and 90 mb over the Central United States on 12 December 1965.

to be some areas quite clear of the emitter and others where the emitter was observed almost continuously over the entire 12-hour period. A similar analysis for several other levels was carried out. There was little apparent similarity between the separate levels. Other meteorological data for the 12 December 1965 period are included in Appendix D.

Most recent literature (Rosen [47]) treats the stratospheric aerosol as a relatively constant feature, one that varies by a factor of two or three in its concentration at an altitude of 16 or 18 km. Very few firm data on this variability are actually available. Grams and Fiocco [19] found an average mass concentration of 8×10^{-19} gm/cc at 16 km, with an RMS variation of 33%. Elterman [15] used a searchlight method to determine that, at an altitude of about 18 to 19 km, the aerosol absorption coefficient has a standard deviation of about 50%. Rosen [46] does not give any figures on the variability, but considers a 400% difference between ascent and descent data for his instrument as providing "fair" agreement. Kondratiev [24], using solar extinction profiles to infer the aerosol concentrations, spoke of the 'repeatability' of occurrence of aerosol layers, with a typical value of 50% for altitudes above 14 km. Murcray [42] has observed that the emission may vary on the time scales of the order of minutes at temperate latitudes. Lawrence [32] has noted that the mid-latitude aerosol has a much greater variability than the tropical aerosol which he observed with his shipboard LIDAR during the BOMEX experiment. Our own synoptic-scale data obtained on 12 December 1965 and the daily Line Island time series indicate that some day-to-day variability is present in the tropics, but this variability is more pronounced in the mid-latitudes.

Obviously, neither Rosen's, Kondratiev's, nor our radiometersonde technique is very well suited for the kind of observations which are needed to describe the synoptic features of the stratospheric aerosol. LIDAR techniques are most suitable and should be utilized for measuring such parameters in the future.

Polar Measurements.

Three years of data taken during the polar winter night are available for Byrd Station. In 1962 and 1963 an older model radiometer using a rod thermistor was utilized. The results yielded an excessive value for the downward irradiance at high altitudes. An intercomparison of this radiometer with the new model was carried out in May 1966, and it was shown that if the irradiance values obtained from the old radiometer were normalized to those obtained from the new radiometer at altitudes above 50 mb, the resultant slopes of the downward irradiance would be very similar, and almost identical emitter concentrations could be obtained (see Appendix B). Thus, all three years of Antarctic data are directly comparable.

a. Mean Profiles. The mean annual profiles for β_{abs}, temperature, lapse rate, and frequency of occurrence at Byrd Station for 1962, 1963, and 1964 are presented in Figures 28a and 28b. The most persistent feature is the emitter layer near 45 mb, which is evident in the average β_{abs} curves for all three years. Another small maximum can be observed near 100 mb. The frequency of occurrence profiles show a pronounced peak at 90 mb and well-pronounced minima at 50, 80, and 110 mb for all three years. There are some significant differences between the three years, however. At altitudes above 90 mb there is a significant increase in the mean β_{abs} values from 1962 to 1963 and again from 1963 to 1964. This 100% to 200% increase is difficult to explain in terms of either the lapse rate or temperature profiles which are essentially similar for all three years. The frequency of occurrence in this region increases by about 300% from 1962 to 1963; then remains about the same during 1964, except at the 70-mb level, where it decreases almost back to the 1962 values.

It would be tempting to say that the apparent increase in the emitter can be linked to the eruption of the Agung volcano in March 1963. First, however, let us examine the monthly time series.

b. Monthly Time Series. Since the radiometersonde can be flown only at night, the data from Antarctica are limited to the polar winter from April to September. Monthly mean data for these months for 1962, 1963, and 1964 are presented in Figures 29a through 29d, Figures 30a through 30d, and Figures 31a through 31d, respectively.

For 1962 and 1964, the distribution of the β_{abs} isopleths appears to be chaotic, with few of the well-defined layers that appear in the tropics in evidence. Still, we can detect maximum concentrations at about the 45-mb and 100-mb levels. The β_{abs} analysis for 1963 shows the presence of several layers, primarily at 45 mb but also at 100 mb, 130 mb, and at about 170 mb. The frequency of occurrence time series indicates similar results. It is interesting to note the relationship that exists between temperatures, which become colder as the polar vortex develops, and the maximum values of β_{abs}. In all cases, when the monthly mean β_{abs} exceeds $.3 \times 10^{-7} cm^{-1}$, the temperature is -70°C or colder. No obvious relationships between the lapse-rate structure and the β_{abs} values were noted.

c. Discussion. The Agung eruption occurred in March 1963 on Bali. The volcanic-ash cloud spread rapidly to the west and south and, according to Weinert [56], by mid-April 1963 it covered all of Australia. By the end of April it had reached New Zealand. Viebrock and Flowers [52] report the first

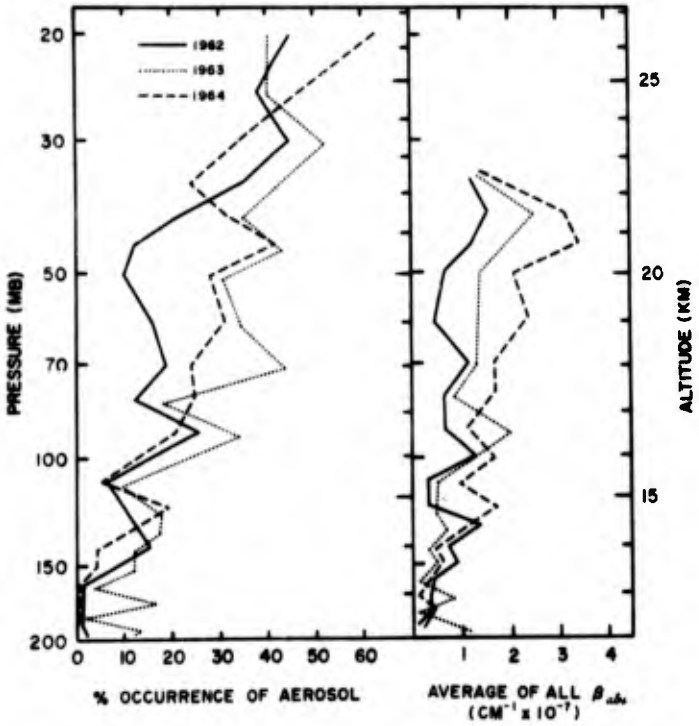

Figure 28a. Mean Antarctic Profiles — Absorption Coefficient ($\beta_{abs} \times 10^{-7} cm^{-1}$) and Percent Frequency of Occurrence.

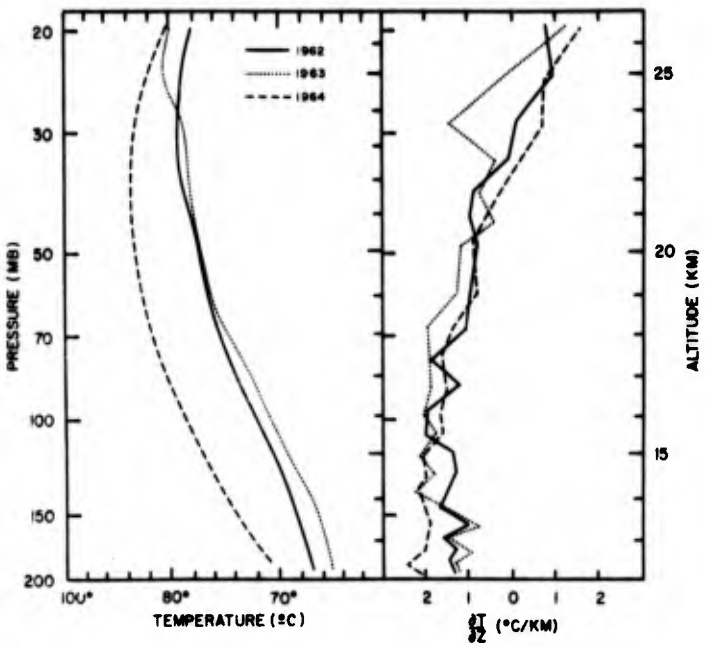

Figure 28b. Mean Antarctic Profiles — Temperature (°C) and Temperature Lapse Rate (°C/km).

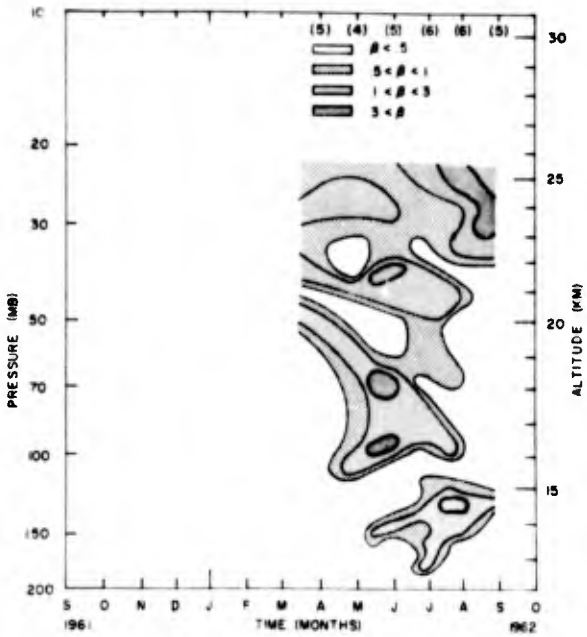

Figure 29a. 1962 Byrd Station Monthly Time Series – Absorption Coefficient ($\beta_{abs} \times 10^{-7} cm^{-1}$).

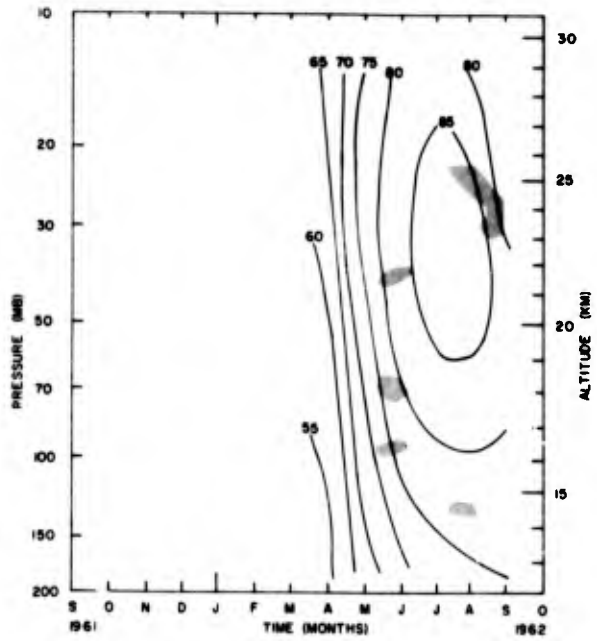

Figure 29c. 1962 Byrd Station Monthly Time Series – Temperature (°C).

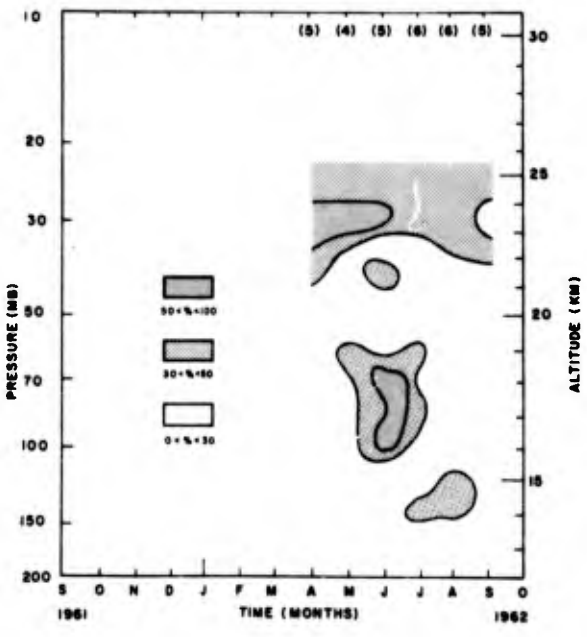

Figure 29b. 1962 Byrd Station Monthly Time Series – Percent Frequency of Occurrence of Emitters.

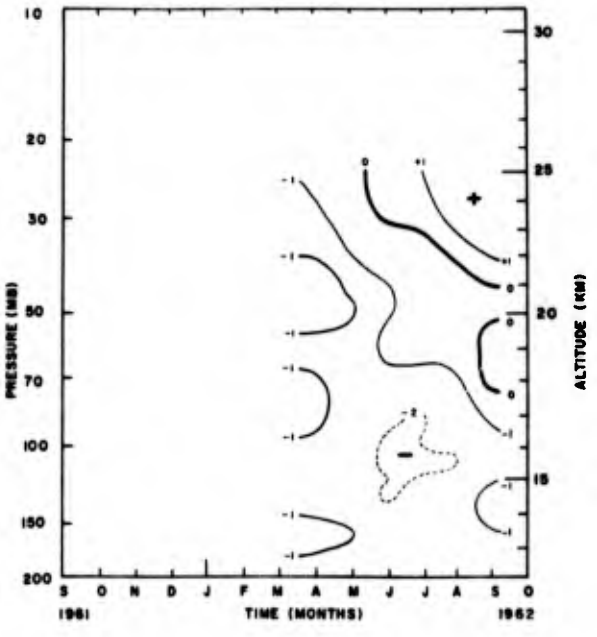

Figure 29d. 1962 Byrd Station Monthly Time Series – Temperature Lapse Rate (°C/km).

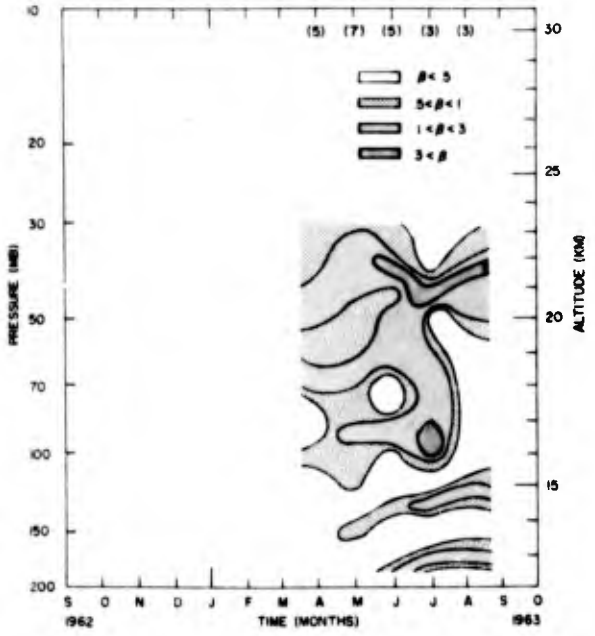

Figure 30a. 1963 Byrd Station Monthly Time Series – Absorption Coefficient ($\beta_{abs} \times 10^{-7} cm^{-1}$).

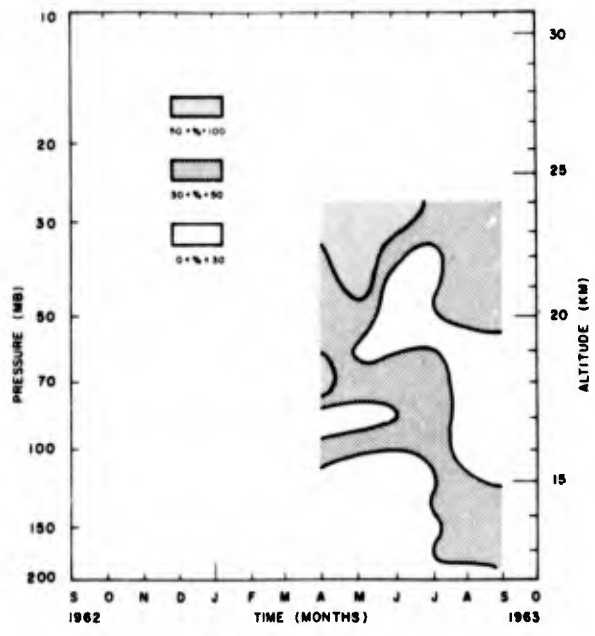

Figure 30b. 1963 Byrd Station Monthly Time Series – Percent Frequency of Occurrence of Emitters.

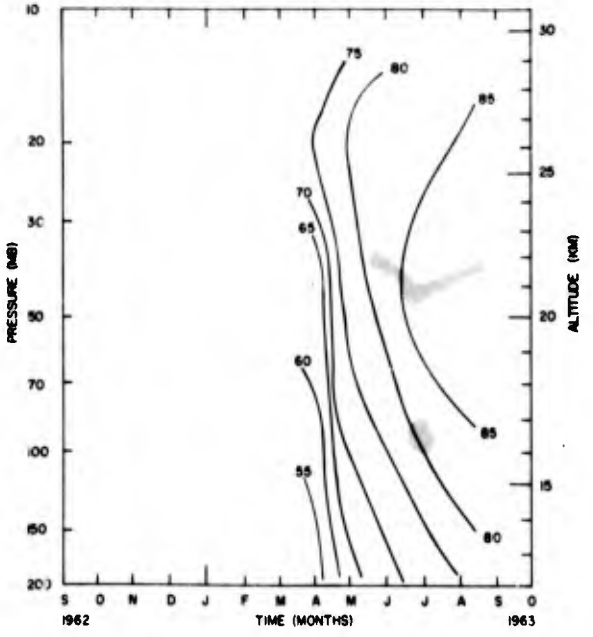

Figure 30c. 1963 Byrd Station Monthly Time Series – Temperature (°C).

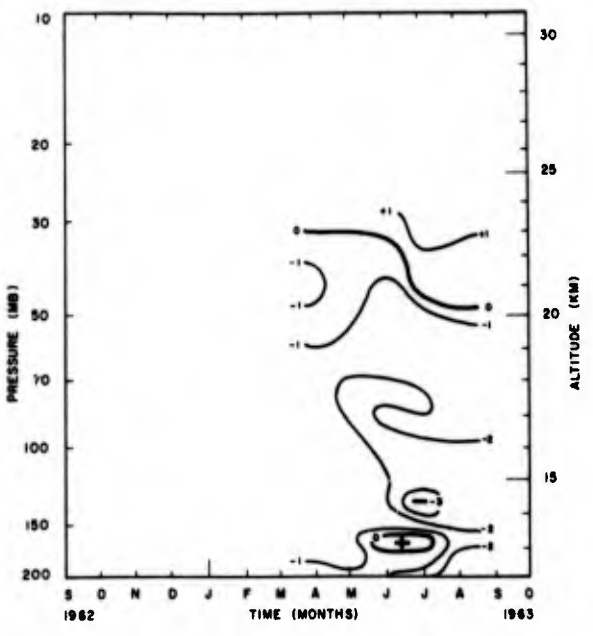

Figure 30d. 1963 Byrd Station Monthly Time Series – Temperature Lapse Rate (°C/km).

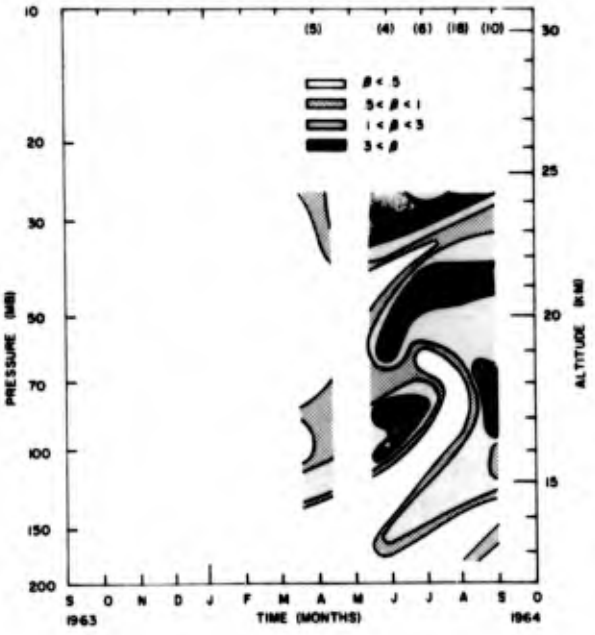

Figure 31a. 1964 Byrd Station Monthly Time Series – Absorption Coefficient ($\beta_{abs} \times 10^{-7} cm^{-1}$).

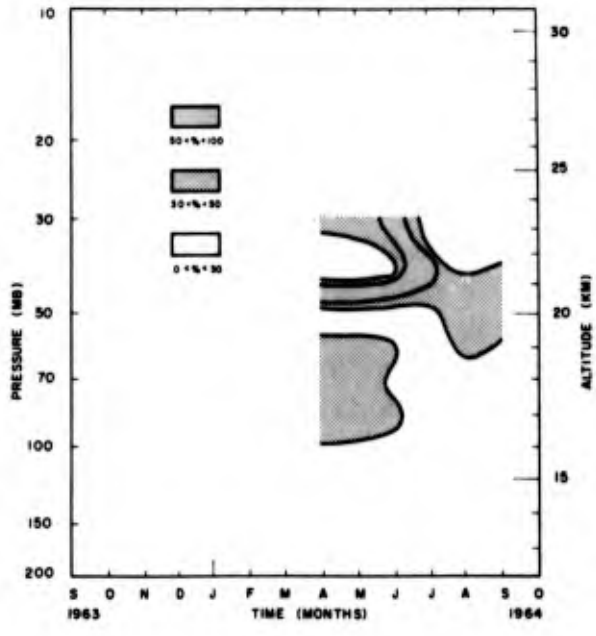

Figure 31b. 1964 Byrd Station Monthly Time Series – Percent Frequency of Occurrence of Emitters.

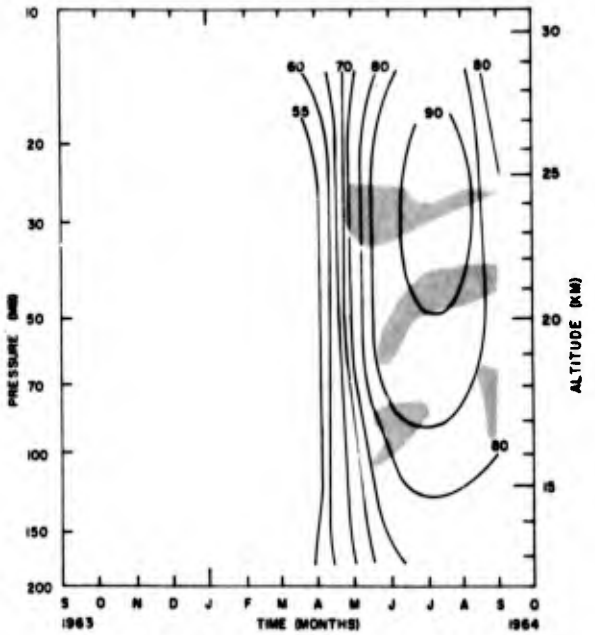

Figure 31c. 1964 Byrd Station Monthly Time Series – Temperature (°C).

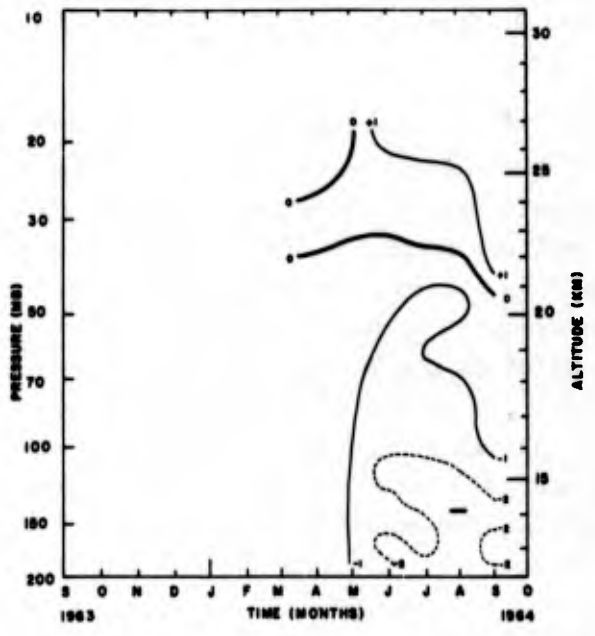

Figure 31d. 1964 Byrd Station Monthly Time Series – Temperature Lapse Rate (°C/km).

sporadic appearances of the volcanic cloud over the South Pole in late November 1963. By mid-December the cloud had become a persistent feature over this region, causing a significant decrease in the intensity of the direct solar radiation at the South Pole. The altitude of this volcanic cloud was estimated by Viebrock and Flowers to be at about the 50-mb level.

The radiometersonde data for 1963 indicate the appearance of a dense emitting layer at 45 mb in June 1963 at Byrd Station (80°S). Other layers appeared in May and June at lower altitudes, indicating the possibility that more than one layer was caused by the volcanic eruption. It must be noted, however, that a similar, even though less well-defined, layer existed at these altitudes in 1962 prior to the eruption. This raises some uncertainties as to whether what is seen in 1963 is actually the aerosol from the volcanic eruption or a seasonal phenomenon associated with the formation of the cold polar-winter vortex. The apparent disagreement with the timing of the arrival of the aerosol as measured by Viebrock and Flowers and our observation also raises some questions. However, Wienert's data for Australia and New Zealand indicate a rapid diffusion of the cloud southward, which may have brought the aerosol to 80°S by June. The continued high turbidity reported by Viebrock and Flowers [52] for the 1964-1965 period does agree substantially with the radiometersonde data for mid-1964 for Byrd Station, which shows several emitting layers, the most prominent of which is at about 45 mb.

Conclusions of Climatology.

The results we have obtained are not completely adequate to describe the climatological characteristics of the stratospheric emitter and some puzzling questions remain to be answered. As expected from theory and from observations made by others, the greatest concentrations of the emitter occur in the tropics between 100 mb and 70 mb. Surprisingly, the frequency of occurrence of the emitter is not significantly greater in the tropics than in the mid-latitudes, about 55% at the maximum levels of concentration. A possible exception to this are the data from the Line Islands which indicate a significantly greater frequency of occurrence in the layer between 110 mb and 90 mb. The mean values of β_{abs} at these altitudes are the same at the Line Islands as at Guam or Canton Island. From the time series for the Line Islands, we see some day-to-day variability in the profiles, with only a few days having none or very little emitter. It is most probable, of course, that some emitter in the tropical stratosphere is always present, but about 20% to 40% of the time the concentrations are below the sensitivity limit of our measurements.

In the mid-latitudes, the emitter layer was found to be, as expected on the basis of previous LIDAR observations, highly variable and much less opaque than in the tropics. As a matter of fact, the term 'layer' may not be applicable in this region and it may be better to speak of emitter clouds, implying discontinuities in the horizontal dimension and variable thickness with various levels

of occurrence in the vertical. On the average, the emitter in the mid-latitudes shows a maximum β_{abs} of $1 \times 10^{-7}cm^{-1}$ at 17 km, a second maximum of $0.5 \times 10^{-7}cm^{-1}$ at 21 km, and a frequency of occurrence of about 55% and 30%, respectively, for the two levels. The synoptic data for 12 December 1965 indicate that a synoptic-scale pattern of the aerosol distribution exists, but no meaningful relationship with conventional meteorological parameters could be established. A determination of the isentropic trajectories of the air parcels which contained the aerosol is one technique which was not explored, but which may prove to be a useful tool to determine whether the aerosol was advected from the tropics or was formed in the mid-latitudes by some local processes.

The Antarctic data indicate that while the frequency of occurrence of the emitter is low, typically 20% to 40%, the values of β_{abs} are about equal to or somewhat greater than those observed in the mid-latitudes. The maximum values of β_{abs} and frequencies of occurrence appear at greater altitudes than either in the tropics or in the mid-latitudes, mostly in the region between 70 and 45 mb. Since the Antarctic data spanned the 1962-1964 period and indicated a trend towards increasing turbidity, an attempt was made to show that this was due to the injection of volcanic ash by the Agung eruption. Such a relationship, however, is very tenuous and a positive statement to the effect that we were observing the volcanic cloud is not justified.

Several researchers, including Grams and Fiocco at Boston, had noticed a modest decrease in the LIDAR backscatter from the 17-mb region during the 1964-1965 period. Our data for Washington do not indicate such trend over the 10-month period of observations. This could mean that we are not observing the same phenomenon as those who are utilizing optical techniques, at least in the mid-latitudes, or that we had insufficient data to obtain significant results. If both sets of observations are correct, one must conclude that the size distribution of the aerosol in the mid-latitudes was changing during this period, with a pronounced removal of particles greater than 0.1μ.

A possible long-term decrease in the stratospheric emitter appears in our data from the tropics. The 1967 mean profiles from the Line Islands show much lower concentrations and frequencies of occurrence at altitudes above 18 km than were observed at Guam or Canton Island during the 1964-1965 period. It is possible that these differences in the mean profiles may actually represent the prevailing differences which exist between the region at 150°W and 150 to 170°E, rather than a real decrease of the stratospheric aerosol. Vincent [53] has indicated that temperature and wind fields exhibited a longitudinal dependence in the tropical stratosphere, and this may also be the case for stratospheric emitters. On the basis of these limited data, it is impossible to establish unambiguously the presence of any long-term trends in emitter concentrations in the tropics or the mid-latitudes. However, a definite increase in the stratospheric aerosol over Antarctica for the 1962-1964 period was observed.

SECTION G — SUMMARY OF FINDINGS

This study has established that the downward directed infrared irradiance in the lower stratosphere, as measured by the Suomi-Kuhn net radiometer, cannot be ascribed exclusively to the emissions of carbon dioxide, ozone, and water vapor. An additional gray emitter was therefore postulated to exist in this region to account for the observed downward infrared irradiance. Intercomparisons between LIDAR data from Jamaica and radiometersonde data from Miami were conducted on two separate occasions. Results indicate that the regions of maximum backscatter and maximum gray emitter occurred at the same altitudes. On the basis of this evidence, it is assumed that this emitter is probably an aerosol, although there may also be a gas, such as HNO_3, present with the aerosol at these levels.

A size distribution for this aerosol was postulated which would account for the results obtained by both the LIDAR and radiometersonde techniques. The size distribution most likely to satisfy these conditions includes a small number of particles with radii greater than 0.1μ, having a power-law distribution, plus a much greater number of small particles with a radius smaller than 0.01μ.

The mass concentration of this aerosol, assuming a density of 2 gm/cm^3, has been calculated to be 8×10^{-11} gm/cm^3 at 70 mb and 3×10^{-11} at 30 mb. This corresponds to a mixing ratio of 6×10^{-7} gm/gm, which is of the same order of magnitude as the water vapor concentration of $\sim 10^{-6}$ gm/gm measured at these altitudes. Since an inverse relationship between the aerosol and water vapor was observed on one of the two occasions studied, it is tempting to speculate that the aerosol is hygroscopic and absorbs some of the water vapor present.

A climatology of the emitter based on some 400 radiometersonde ascents indicates that the stratospheric emitter is a global phenomenon. The greatest concentrations and the highest frequencies of occurrence are found in the tropics at about 16 to 18 km altitude. Typical values of β_{abs} at 80 mb are about $5 \times 10^{-7} cm^{-1}$. In the mid-latitudes, the concentration is only about 10% to 20% of that found in the tropics, while the frequency of occurrence is about the same, with typical values of about 50% near 80 mb. In the polar regions, where data representative only of the Antarctic winter were available, the maximum values of the absorption coefficient were found at 45 mb, with the β_{abs} values about 50% of those in the tropics. The average value for the total absorption, $\beta_{abs} \cdot x$, was 0.20 for the tropics, 0.05 for the mid-latitudes, and 0.10 for the polar region. On any given day, however, the total absorption may depart by ± 100% from these average values.

On the basis of these global data, it is possible to postulate that the tropical stratosphere is a region of high emitter concentration. Perhaps the aerosol is formed in the tropics as the result of reactions between ammonia and sulfer dioxide such as those proposed by Scott and Lamb [49]. Such hygroscopic

aerosols would grow in the tropical stratosphere, then evaporate as they were transported poleward in air which is warmed adiabatically as it sinks to higher pressures along isentropic surfaces. Moving into the polar-winter vortex, these gases may recondense to form the observed secondary concentration maximum, provided sufficient adiabatic cooling takes place as the isentropes slope upward within the vortex.

Time series of daily observations in the Pacific area indicate that in the tropics the stratospheric emitter is a persistent phenomenon, a fact also noted by investigators using LIDAR techniques. It appears to be more variable in the mid-latitudes, where profiles obtained three to four hours apart indicate rapidly changing concentrations. An analysis of synoptic-density emitter data obtained over the Central United States on 12 December 1965 indicated that the emitter seemed to be randomly distributed and was not apparently related to conventional meteorological parameters.

On the basis of our data it has not been possible to detect any long-term trends in the concentration of the stratospheric emitter for the mid-latitudes or for the tropics. However, the emitter concentration over Antarctica appeared to increase significantly during the 1962-1964 period. While the exact reason for this increase is not known, it may be related to the Agung volcano eruption in March of 1963.

SECTION H — REFERENCES

[1] Bushnell, R. H., and Suomi, V. E.: "Experimental Flight Verification of the Economical Net Radiometer," J. Geophys. Res., Vol. 66, No. 9, pp. 2843-2848, 1961.

[2] Cadle, R. D., et.al.: "Trace Constituents in the Vicinity of Jet Streams," J. Appl. Meteorol., Vol. 8, pp. 348-356, 1969.

[3] Calfee, R. F., and Gates, D. M.: "Calculated Slant Path Absorption and Distribution of Atmospheric Water Vapor," Appl. Optics, Vol. 5, pp. 287-292, 1966.

[4] Clemesha, B. R., Kent, G. S., and Wright, R. W. H.: "Laser Probing of the Lower Atmosphere," Nature, Vol. 209, pp. 184-185, 1966.

[5] Cole, A. E., Court, A., and Kantor, A. J.: "Model Atmospheres," Chap. 2, pp. 2-1 through 2-22, in: Handbook of Geophysics and Space Environments, Edited by S. Valley, McGraw-Hill, New York, 1965.

[6] Collis, R. T. H., and Ligda, M. G. H.: "Note on LIDAR Observations of Particulate Matter in the Stratosphere," J. Atmospheric Sci., Vol. 23, pp. 255-257, 1966.

[7] Cox, S. K.: A Radiation Model in Which the Effects of Clouds are Simulated from Moisture and Temperature Parameters. PhD dissertation, Dept. of Meteorology, University of Wisconsin, Madison, 1967.

[8] Darkow, G. L.: A Study of Infrared Radiation Measurements in the Vicinity of the Subtropical Tropopause. PhD dissertation, Dept. of Meteorology, University of Wisconsin, Madison, 1964.

[9] de Bary, E., and Rossler, F.: "Size Distributions of Atmospheric Aerosols Derived from Scattered Radiation Measurements Aloft," J. Geophys. Res., Vol. 71, No. 4, pp. 1011-1016, 1966.

[10] Deirmendjian, D., Clasen, R., and Viezee, W.: "Mie Scattering with Complex Index of Refraction," J. Optical Soc. Amer., Vol. 51, pp. 620-633, 1961.

[11] Driving, A., et.al.: "Photometric Analysis of Photographs of the Twilight Aureole Obtained from the Spaceship Vostok-6," Izv. Atmospheric and Oceanic Phys., Vol. 2, pp. 1046-1054, 1966.

[12] Elsasser, W. M., and Culbertson, M. F.: "Atmospheric Radiation Tables" in: Meteorological Monograph 23, American Meteorological Society, Boston, Mass., p. 43, 1960.

[13] Elterman, L.: "Seasonal Trends of Temperature, Density and Pressure in the Stratosphere Obtained with Searchlight Probing Techniques," Geophys. Res. Paper No. 29, Air Force Cambridge Research Center, Cambridge, Mass., 1954.

[14] Elterman, L.: "An Atlas of Aerosol Attenuation and Extinction Profiles for the Troposphere and Stratosphere," Environmental Res. Paper No. 241, Optical Physics Laboratory, Air Force Cambridge Research Laboratories, L. G. Hanscom Field, Mass., 1966.

[15] Elterman, L., Wexler, R., and Chang, D. T.: "Features of Tropospheric and Stratospheric Dust," Appl. Optics, Vol. 8, pp. 893-903, 1969.

[16] Fried, P. M.: Personal Communication (1970).

[17] Friend, J. P.: "Properties of the Stratospheric Aerosol," Tellus, Vol. 18, pp. 465-473, 1966.

[18] Goody, R. M.: Atmospheric Radiation, Oxford University Press, London, p. 436, 1964.

[19] Grams, G. W., and Fiocco, G.: "Stratospheric Aerosol Layer During 1964 and 1965," J. Geophys. Res., Vol. 72, No. 14, pp. 3523-3542, 1967.

[20] Houghton, J. T.: "The Effect of Contamination on Spectroscopic Determinations of Stratospheric Water Vapor," Quart. J. Roy. Meteorol. Soc., Vol. 92, pp. 281-283, 1966.

[21] Johnson, D. R.: "The Effect of Bias and Random Radiometersonde Temperature Errors in the Estimation of Atmospheric Downward, Upward, Net and Equivalent Infrared Irradiance," J. Geophys. Res., Vol. 71, No. 24, pp. 5815-5825, 1966.

[22] Junge, C. E., Chagnon, C. W., and Manson, J. E.: "Stratospheric Aerosols," J. Meteorol., Vol. 18, pp. 81-107, 1961.

[23] Junge, C. E.: Airchemistry and Radioactivity. International Geophysical Series, Vol. 4, Academic Press, Inc., New York, 1963.

[24] Kondratiev, R. Y., et.al.: "Direct Solar Radiation Up to 30 Km and Stratification of Attenuation Components in the Stratosphere," Appl. Optics, Vol. 6, pp. 197-207, 1967.

[25] Kosters, J. J., Kyle, T. G., and Murcray, D. G.: "Attenuation of the Direct Solar Beam by Aerosols," J. Geophys. Res., Vol. 74, No. 13, pp. 3380-3383, 1969.

[26] Kent, G. S., Clemesha, B. R., and Wright, R. W.: "High Altitude Atmospheric Scattering of Light from a Laser Beam." J. Atmospheric and Terrest. Phys., Vol. 29, pp. 169-181, 1967.

[27] Kroening, L. J.: "Atmospheric Small Ions and Dust," in: Annual Progress Rept., Atmospheric Physics Program, University of Minnesota, 1964.

[28] Kuhn, P. M.: "Soundings of Observed and Computed Infrared Flux," J. Geophys. Res., Vol. 68, No. 5, pp. 1415-1420, 1963.

[29] Kuhn, P. M., and Suomi, V. E.: Radiometersonde Technical Manual, Dept. of Meteorology, University of Wisconsin, Madison, 1 October 1964.

[30] Kuhn, P. M., and Johnson, D. R.: "Improved Radiometersonde Observations of Atmospheric Infrared Irradiance," J. Geophys. Res., Vol. 71, No. 2, pp. 367-373, 1966.

[31] Kuhn, P. M., and Cox, S. K.: "Radiometric Inference of Stratospheric Water Vapor," J. Appl. Meteorol., Vol. 6, pp. 142-149, 1967.

[32] Lawrence, J. D.: Personal Communication (1970).

[33] Lettau, H.: "Diffusion in the Upper Atmosphere," in: Compendium of Meteorology, Boston, Mass., pp. 320-333, 1951.

[34] Lettau, H.: "Theoretical Notes on the Dynamics of the Equatorial Atmosphere," Beitr. zur Phys. der Atmospäre, Vol. 29, pp. 107-122, 1956.

[35] Madolen, R. A., and Zipser, E. J.: "Multilayered Structure of the Wind Over the Equatorial Pacific During the Line Islands Experiment," J. Atmospheric Sci., Vol. 27, No. 2, pp. 336-342, 1970.

[36] Mastenbrook, H. J.: "Water Vapor Observations at Low, Middle and High Latitude During 1964 and 1965," NRL Report 6447, Naval Research Laboratory, Washington, D. C., 1966.

[37] Miller, A. J.: "Vertical Motion Atlas for the Lower Stratosphere During the IGY," Rep. No. 16, M.I.T., Dept. of Meteorology, Planetary Circulations Project, AF (604)-5223, AT (30-1) 2241, 1966.

[38] Mossop, S. C.: "Volcanic Dust Collected at an Altitude of 20 Km," Nature, Vol. 203, pp. 824-827, 1964.

[39] Murcray, D. G., Murcray, F. H., and Williams, W. J.: "Comparison of Experimental and Theoretical Slant Path Absorptions in the Region from 1400 to 2500 cm^{-1}," J. Optical Soc. Amer., Vol. 55, pp. 1239-1246, 1965.

[40] Murcray, D. G., Murcray, F. H., and Williams, W. J.: "Further Data Concerning the Distribution of Water Vapour in the Stratosphere," Quart. J. Roy. Meteorol. Soc., Vol. 92, pp. 159-161, 1966.

[41] Murcray, D. G., et.al.: "Presence of HNO_3 Vapor in the Upper Atmosphere," J. Optical Soc. Amer., Vol. 59, pp. 1131-1134, 1969.

[42] Murcray, D. G., Brooks, J. N., and Williams, W. J.: Flight Data Summary Report, Physics Dept., University of Denver, Denver, Colorado, January 1970.

[43] Newkirk, G. Jr., and Eddy, J. A.: "Light Scattering by Particles in the Upper Atmosphere," J. Atmospheric Sci., Vol. 21, No. 1, pp. 35-60, 1964.

[44] Paltridge, G. W.: "Stratospheric Small Ion Density Measurements from a High-Altitude Jet Aircraft," J. Geophys. Res., Vol. 71, No. 8, pp. 1945-1952, 1966.

[45] Pilipowskyj, S., et.al.: "Investigation of the Stratospheric Aerosol by Infrared and LIDAR Techniques," J. Geophys. Res., Vol. 73, No. 24, pp. 7553-7560, 1968.

[46] Rosen, J. M.: "Simultaneous Dust and Ozone Soundings Over North and Central America," School of Physics and Astronomy, University of Minnesota, Report AP-25, August 1967 (AD-658546).

[47] Rosen, J. M.: "Simultaneous Dust and Ozone Soundings Over North and Central America," J. Geophys. Res., Vol. 73, No. 2, pp. 479-486, 1968.

[48] Rosenberg, G. V., (ed): Searchlight Beam in the Atmosphere. Acad. of Sci. USSR, Moscow, 1960. (Partial translation, AID Rept. 62-126, August 28, 1962, AID work assignment No. 35, OAR No. 2, Task 5.)

[49] Scott, W. D., and Lamb, D.: "Two Models of the Stratospheric Sulfate Layer." Paper presented at the National fall meeting of the American Geophysical Union, San Francisco, California, 1969.

[50] Suomi, V. E., and Kuhn, P. M.: "An Economical Net Radiometersonde," Tellus, Vol. 10, pp. 160-163, 1958.

[51] van de Hulst, H. C.: Light Scattering by Small Particles, Wiley and Sons, New York, p. 287, 1957.

[52] Viebrock, H. J., and Flowers, E. C.: "Comments on the Recent Decrease in Solar Radiation at the South Pole," Tellus, Vol. 20, pp. 400-411, 1968.

[53] Vincent, D. G.: "Mean Meridional Circulations in the Northern Hemisphere Lower Stratosphere During 1964 and 1965," Quart. J. Roy. Meteorol. Soc., Vol. 94, pp. 333-349, 1968.

[54] Volz, F. E., and Goody, R. M.: "The Intensity of the Twilight and Upper Atmospheric Dust," J. Atmospheric Sci., Vol. 19, pp. 385-406, 1962.

[55] Volz, F. E.: "Twilight and Stratospheric Dust Before and After the Agung Eruption," Appl. Optics, Vol. 8, pp. 2505-2517, 1969.

[56] Weinert, R. A.: "The Movement and Dispersion of Volcanic Dust from the Eruption of Mt. Agung, Bali, 17 March 1963," Australian Meteorol. Mag., Vol. 15, No. 4, pp. 225-229, 1967.

[57] Wexler, H.: "Spread of the Krakatoa Volcanic Dust Cloud as Related to the High-Level Circulation," Bull. Amer. Meteorol. Soc., Vol. 32, No. 2, pp. 48-51, 1951.

[58] Zander, R.: "Moisture Contamination at Altitude by Balloon and associated Equipment," J. Geophys. Res., Vol. 71, No. 15, pp. 3775-3778, 1966.

Appendix A

TEMPERATURE, OZONE, AND WATER VAPOR MODELS

Temperature Models.

It was necessary to postulate a temperature distribution to an altitude of 0.1 mb in order to carry out the radiative transfer calculations. The free-air temperature measured by the radiometersonde during each ascent was, in all cases, available to an altitude of 50 mb, sometimes as high as 5 mb. These measured air temperatures were supplemented as necessary by the temperature distributions shown in Table A-1.

TABLE A-1

Pressure (mb)	Temperature (°C)	
	Tropics & Mid-Latitudes	Antarctica
.100	-40.0	-40.0
.300	-2.0	-10.0
.600	7.0	-20.0
1.000	4.0	-30.0
2.000	-10.0	-50.0
3.000	-20.0	-60.0
5.000	-35.0	-65.0
7.000	-38.0	-70.0
10.000	-41.5	-75.0
15.000	-47.5	-80.0
20.000	-52.5	-82.0
25.000	-57.5	-82.0
30.000	-59.0	-82.0
35.000	-61.0	-82.0
40.000	-62.5	-82.0
45.000	-63.5	-82.0

Ozone Models.

The ozone distributions used in the radiative transfer calculations are shown in Table A-2.

TABLE A-2

Pressure (mb)	Ozone Concentration (cm O_3/km STP)	
	Tropics & Mid-Latitudes	Antarctica
.100	.0000	.0000
.300	.0000	.0000
.600	.0000	.0000
1.000	.0000	.0000
2.000	.0020	.0010
3.000	.0010	.0010
5.000	.0050	.0030
7.000	.0070	.0050
10.000	.0100	.0080
15.000	.0200	.0120
20.000	.0300	.0160
25.000	.0300	.0180
30.000	.0300	.0210
35.000	.0300	.0220
40.000	.0200	.0220
45.000	.0150	.0220
50.000	.0120	.0200
60.000	.0150	.0200
70.000	.0100	.0260
80.000	.0080	.0220
90.000	.0060	.0200
100.000	.0050	.0180
110.000	.0040	.0160
120.000	.0030	.0140
130.000	.0020	.0120
140.000	.0010	.0100
150.000	.0010	.0080
160.000	.0000	.0060
170.000	.0000	.0040
180.000	.0000	.0030
190.000	.0000	.0020
200.000	.0000	.0010

Water Vapor Models.

Five different models of the stratospheric water-vapor distribution were used in the radiative transfer calculations; they are given in Table A-3. Model #1 and Model #4 represent the extreme dry and moist conditions. Calculations for the distribution of the infrared emitters were made using Model #2 for mid-latitude ascents, Model #3 for tropical ascents, and Model #5 for the Antarctic flights.

TABLE A-3

Pressure (mb)	Water Vapor Mixing Ratio (gm/kg)				
	Model #1 (dry)	Model #2 (mid-lat)	Model #3 (trop)	Model #4 (moist)	Model #5 (polar)
.100	.0000	.0000	.0000	.0000	.0000
.300	.0000	.0000	.0000	.0000	.0000
.600	.0000	.0000	.0000	.0000	.0000
1.000	.0000	.0000	.0000	.0000	.0000
2.000	.0020	.0030	.0030	.0500	.0030
3.000	.0020	.0040	.0040	.0500	.0040
5.000	.0020	.0040	.0040	.0500	.0040
7.000	.0020	.0040	.0040	.0500	.0040
10.000	.0020	.0040	.0040	.0500	.0040
15.000	.0010	.0030	.0030	.0500	.0030
20.000	.0010	.0030	.0030	.0500	.0030
25.000	.0010	.0030	.0030	.0400	.0030
30.000	.0010	.0030	.0030	.0350	.0030
35.000	.0010	.0030	.0030	.0300	.0030
40.000	.0010	.0030	.0030	.0250	.0030
45.000	.0010	.0030	.0030	.0220	.0030
50.000	.0010	.0030	.0030	.0200	.0030
60.000	.0010	.0030	.0030	.0180	.0030
70.000	.0010	.0030	.0030	.0150	.0030
80.000	.0010	.0030	.0030	.0130	.0030
90.000	.0010	.0030	.0030	.0110	.0030
100.000	.0010	.0030	.0030	.0100	.0030
110.000	.0010	.0030	.0040	.0100	.0030
120.000	.0020	.0030	.0050	.0110	.0030
130.000	.0020	.0030	.0070	.0130	.0030
140.000	.0020	.0040	.0100	.0180	.0040
150.000	.0020	.0050	.0130	.0220	.0040
160.000	.0030	.0070	.0160	.0260	.0050
170.000	.0030	.0100	.0200	.0320	.0060
180.000	.0040	.0130	.0250	.0400	.0060
190.000	.0040	.0160	.0320	.0500	.0070
200.000	.0040	.0200	.0400	.0600	.0080

Appendix B

RADIOMETER INTERCOMPARISON

An intercomparison of several models of the Suomi-Kuhn net radiometer was conducted at Green Bay on 26 May 1966. Two of the four radiometer models flown on this occasion are the models which provided the data for this study. The older models of this radiometer were used in Antarctica during the 1962-1963 period; the newer models (see Kuhn and Johnson [30]) were used to obtain all the other data used in this study.

In Figure B-1 we see that the downward irradiances measured by the two radiometers in question are significantly different. However, if the irradiance profile measured by the older radiometer is normalized to that of the new model at 10 mb, the profiles become almost identical. Since the infrared emitter profiles calculated on the basis of these measurements are dependent on the rate of change with height rather than the absolute magnitude of the downward irradiance, similar aerosol profiles could thus be expected. From Figure B-1 we see that the calculated emitter profiles based on either radiometer are very similar.

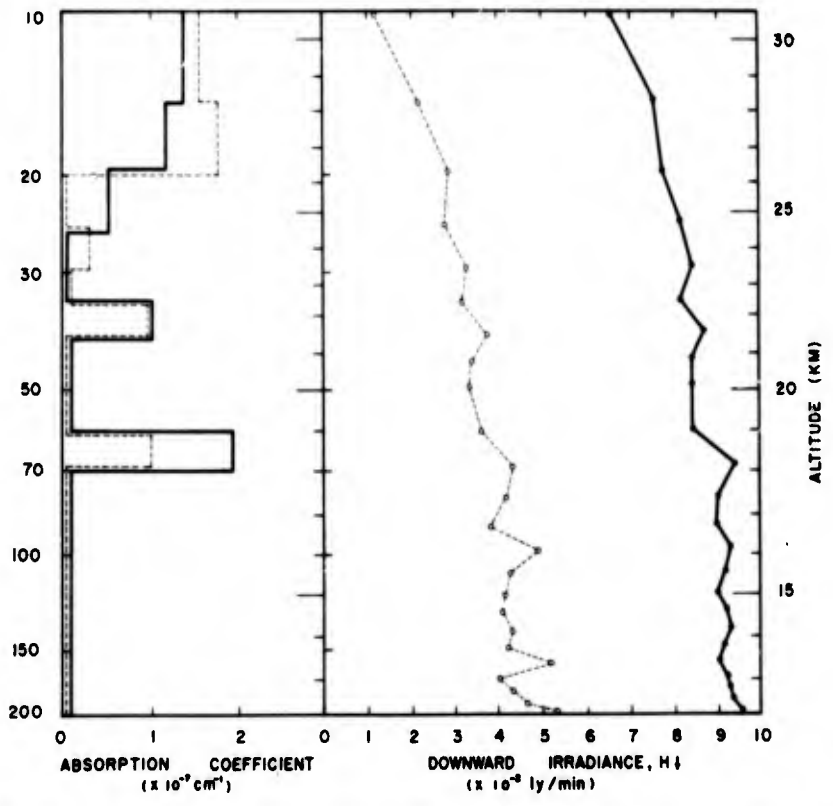

Figure B-1. Absorption Coefficient Profiles as Measured by Old and New Model Radiometers During the 26 May 1966 Intercomparison at Green Bay.

Appendix C

MEAN MONTHLY WIND DATA

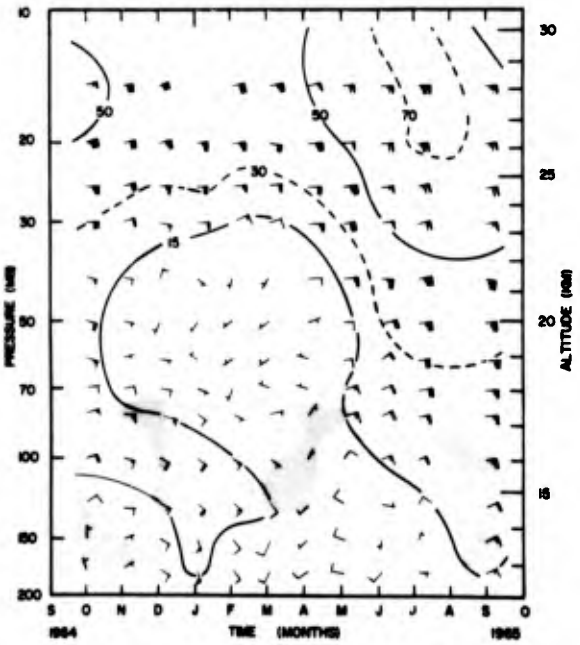

Figure C-1. Guam Monthly Time Series — Winds.

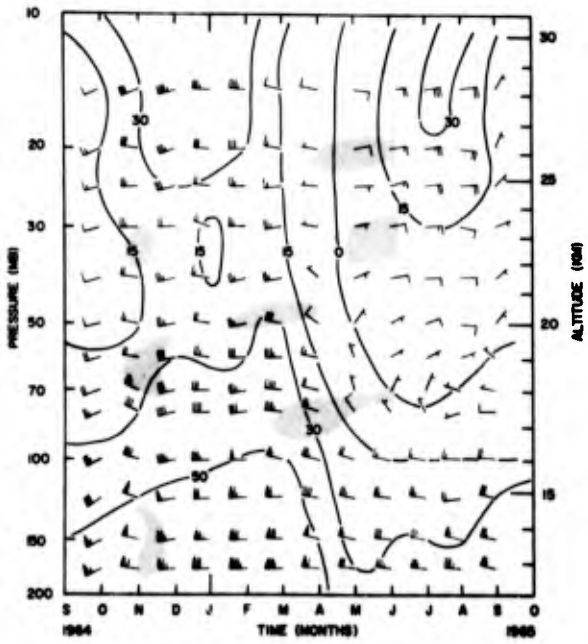

Figure C-3. Washington Monthly Time Series — Winds.

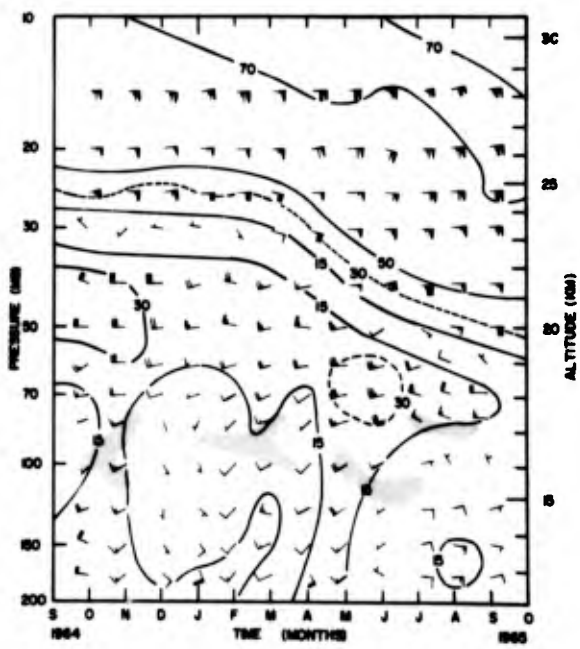

Figure C-2. Canton Island Monthly Time Series — Winds.

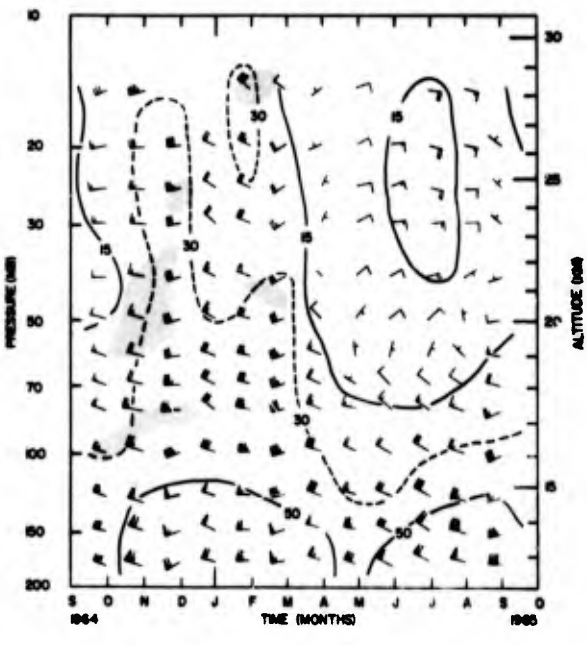

Figure C-4. Green Bay Monthly Time Series — Winds.

Appendix D

SUPPLEMENTARY DATA FOR THE LINE ISLANDS

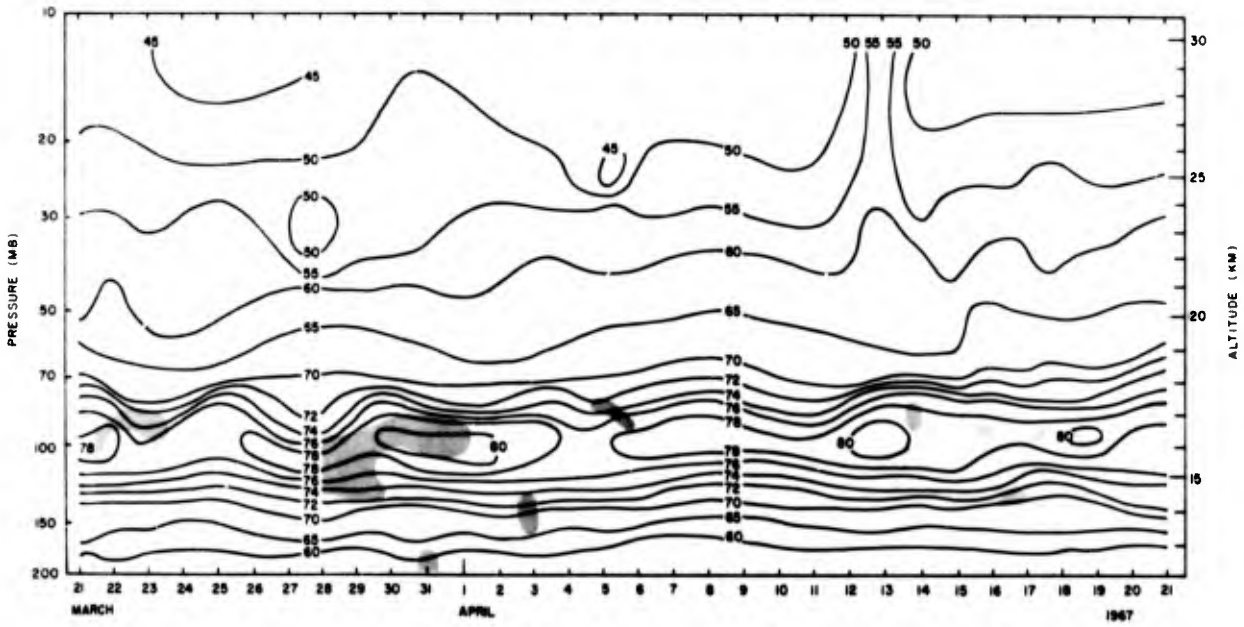

Figure D-1. Christmas Island Daily Time Series — Temperature (°C).

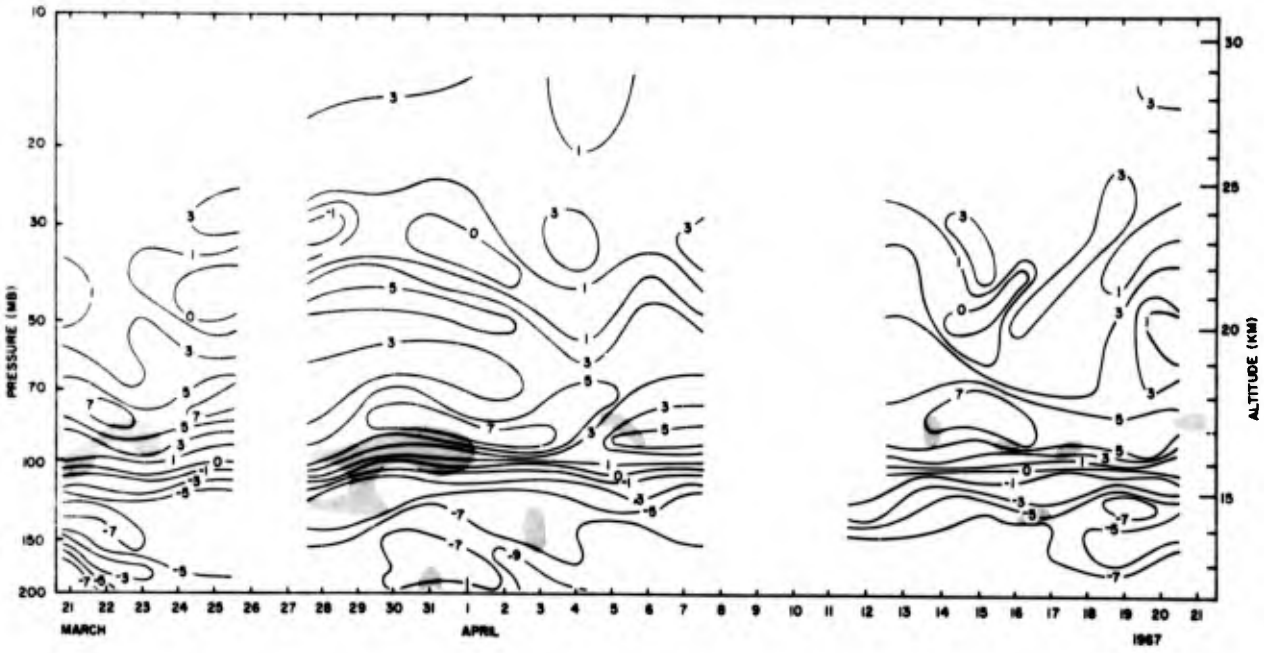

Figure D-2. Christmas Island Daily Time Series — Temperature Lapse Rate (°C/km).

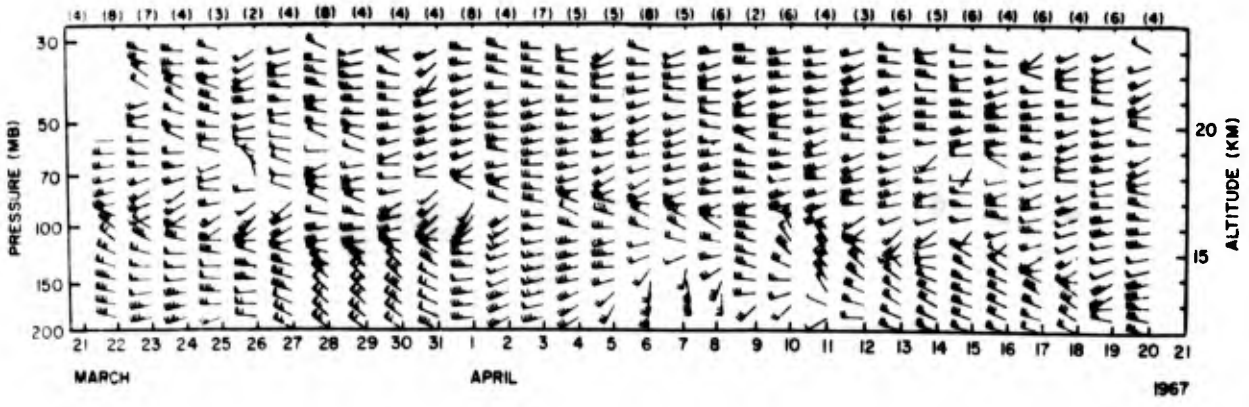

Figure D-3. Christmas Island Daily Time Series — Winds.

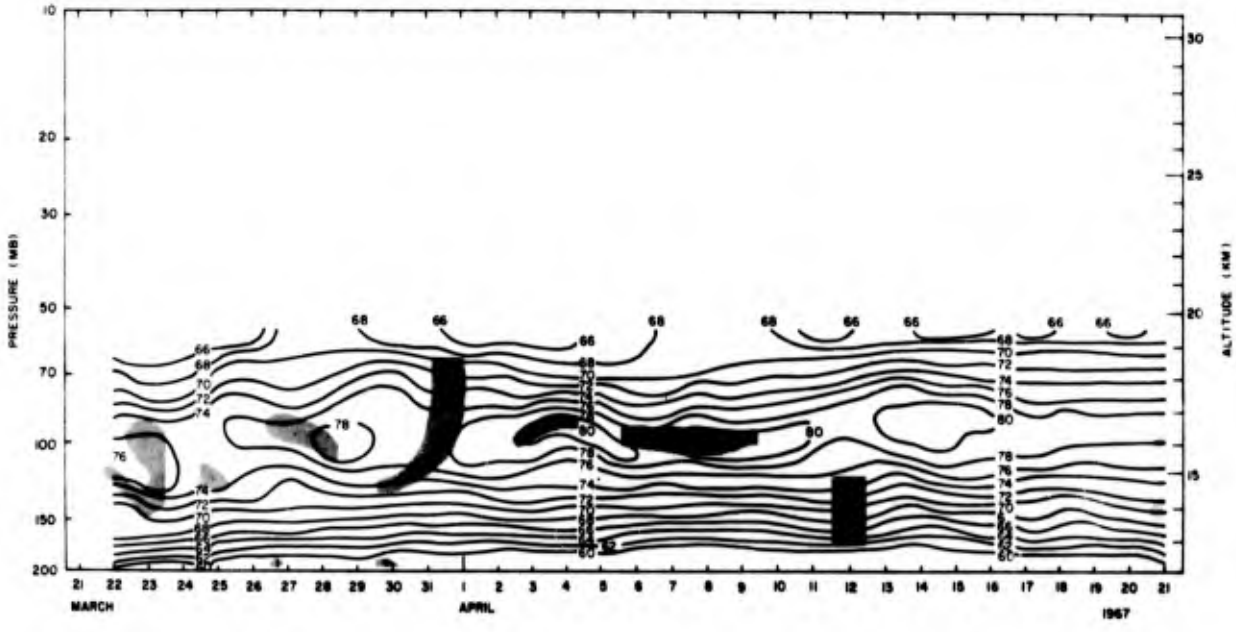

Figure D-4. Palmyra Island Daily Time Series — Temperature (°C).

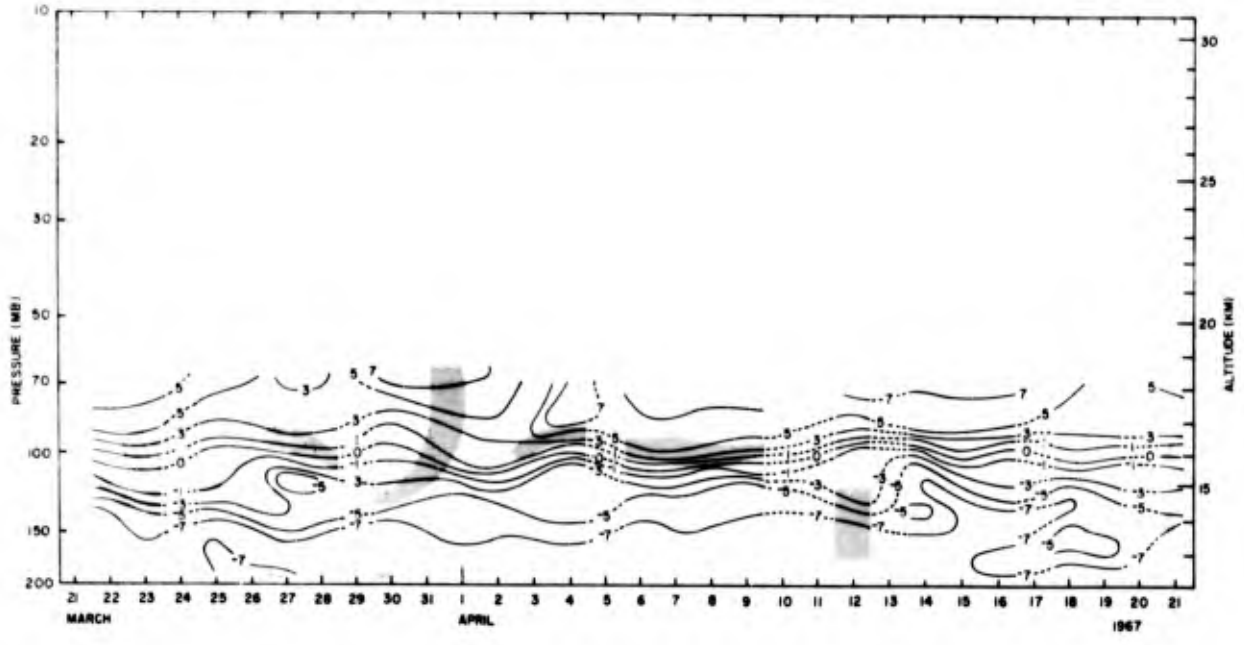

Figure D-5. Palmyra Island Daily Time Series — Temperature Lapse Rate (°C/km).

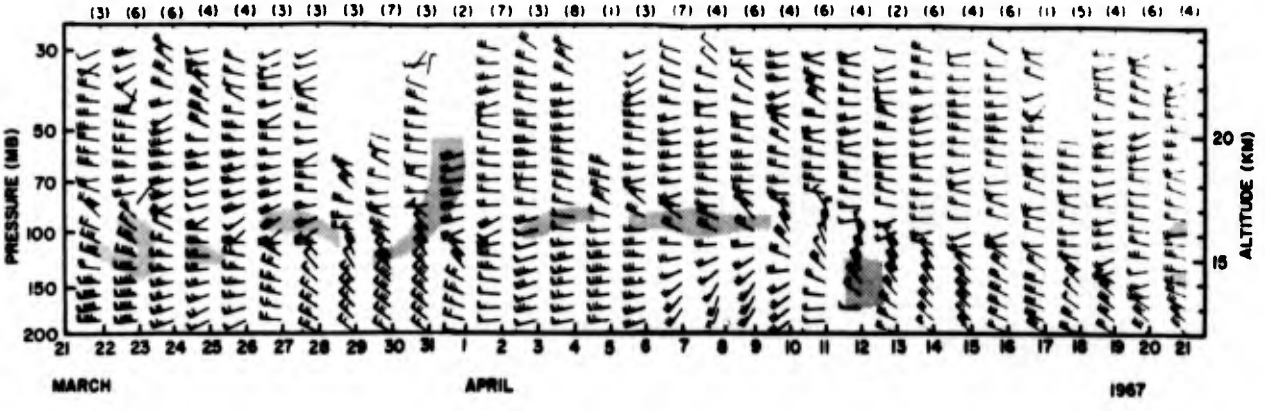

Figure D-6. Palmyra Island Daily Time Series — Winds.

Appendix E

SUPPLEMENTARY DATA FOR THE 12 DECEMBER 1965 FLIGHTS

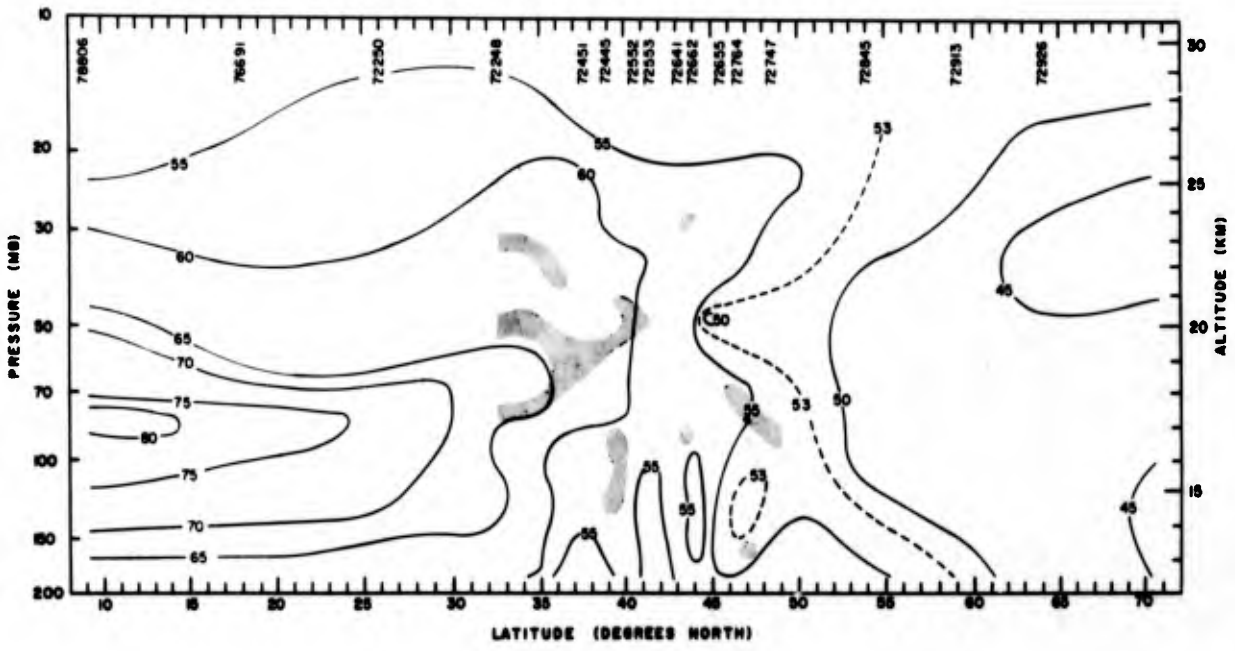

Figure E-1. Central United States Latitudinal Cross-Section of the Temperature (°C) Field on 12 December 1965.

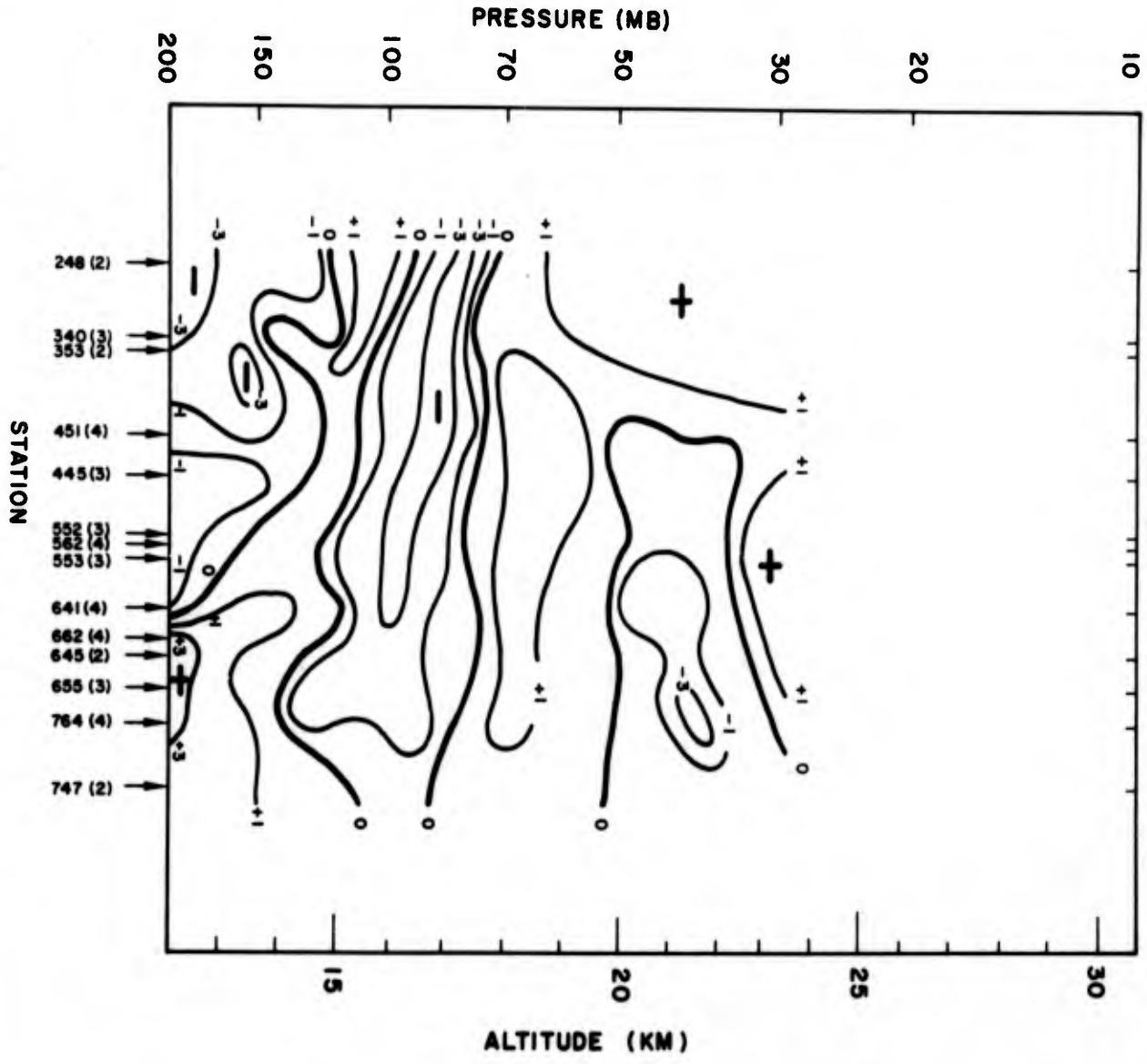

Figure E-2. Central United States Latitudinal Cross-Section of the Temperature Lapse Rate (°C/km) Field on 12 December 1965.

DOCUMENT CONTROL DATA - R & D

(Security classification of title, body of abstract and indexing annotation must be entered when the overall report is classified)

1. ORIGINATING ACTIVITY *(Corporate author)*
Hq Air Weather Service (MAC)
Scott AFB, Illinois 62225

2a. REPORT SECURITY CLASSIFICATION
Unclassified

2b. GROUP
N/A

3. REPORT TITLE
A Study of Stratospheric Emitters Based on Infrared Radiometersonde Measurements

4. DESCRIPTIVE NOTES *(Type of report and inclusive dates)*
N/A

5. AUTHOR(S) *(First name, middle initial, last name)*
Serhij Pilipowskyj, Major, USAF
Prof James A. Weinman

6. REPORT DATE	7a. TOTAL NO. OF PAGES	7b. NO. OF REFS
July 1971	58	58

8a. CONTRACT OR GRANT NO.
N/A
b. PROJECT NO.
c.
d.

9a. ORIGINATOR'S REPORT NUMBER(S)
Air Weather Service Technical Report 221

9b. OTHER REPORT NO(S) *(Any other numbers that may be assigned this report)*

10. DISTRIBUTION STATEMENT
Approved for public release; distribution unlimited.

11. SUPPLEMENTARY NOTES
N/A

12. SPONSORING MILITARY ACTIVITY
Hq Air Weather Service (MAC)

13. ABSTRACT

Analysis of downward-directed infrared irradiances measured in the lower stratosphere indicated that reasonable limits on the gaseous components of the atmosphere were not able to account for the irradiances observed between 14 and 24 km. Additional emitters were therefore assumed to exist at these altitudes. Information on the spatial and temporal distributions of the stratospheric emitter was obtained from an analysis of some 400 measurements taken during the 1962-1967 period. The results indicate that while this phenomenon is global in scope, it is most evident in the tropics at altitudes between 15 and 18 km. Time series of daily radiometersonde ascents carried out during the Line Islands Experiment indicated that the emitter has a high persistence in the tropics. A series of synoptic-scale ascents made over the central United States on one night indicated that the emitter has a great variability in the mid-latitudes. No long-term trends in the concentration of the emitter in the tropics or in the mid-latitudes could be determined.

DD FORM 1 NOV 65 1473

14. KEY WORDS	LINK A		LINK B		LINK C	
	ROLE	WT	ROLE	WT	ROLE	WT
Stratospheric Emitters Stratospheric Aerosols Irradiances, Downward						

S AFB, IL 72-19090